

SnO₂ NANOWIRE BASED SUPERCAPACITOR

by

Lingtao Jiang

B.S, Nanjing University, 2015

Submitted to the Graduate Faculty of
Swanson School of Engineering in partial fulfillment
of the requirements for the degree of
Master of Science

University of Pittsburgh

2017

UNIVERSITY OF PITTSBURGH
SWANSON SCHOOL OF ENGINEERING

This thesis was presented

by

Lingtao Jiang

It was defended on

March 30th, 2017

and approved by

Jung-Kun Lee, PhD, Associate Professor

Department of Mechanical Engineering and Materials Science

Markus Chmielus, PhD, Assistant Professor

Department of Mechanical Engineering and Materials Science

Ian Nettleship, PhD, Associate Professor

Department of Mechanical Engineering and Materials Science

Thesis Advisor: Jung-Kun Lee, PhD, Associate Professor

Copyright © by Lingtao Jiang

2017

SnO₂ NANOWIRE BASED SUPERCAPACITOR

Lingtao Jiang, M.S.

University of Pittsburgh, 2017

In this thesis, Tin oxide (SnO₂) nanowires are synthesized via VLS (Vapor-liquid-solid) method on FTO substrates. The effect of Sb doping, Au seed layer thickness and substrate materials on morphology of a nanowire array has been systematically studied.

Also, the electrical and optical properties of a nanowire array such as resistance, transmission and absorption are characterized. Moreover, manganese oxide and nickel oxide are coated on top of SnO₂ nanowires and their electrochemical properties are analyzed. Our results show that Mn-Ni codeposited Sb-doped SnO₂ nanowires are promising material for high performance supercapacitors.

TABLE OF CONTENTS

ACKNOWLEDGMENT	XI
1.0 INTRODUCTION.....	1
2.0 BACKGROUND INFORMATION AND LITERATURE REVIEW.....	4
2.1 SUPERCAPACITOR.....	4
2.1.1 Electrostatic Double-layer Capacitors (EDLC).....	4
2.1.2 Pseudocapacitors	5
2.2 TRANSPARENT AND CONDUCTING OXIDES.....	7
2.2.1 TCOs Development.....	7
2.2.2 Indium tin oxide (ITO).....	8
2.2.3 Tin Dioxide.....	9
2.2.4 Vapor Liquid Solid (VLS) Method for Nanowire Growth	11
2.2.5 Sb Doped SnO₂ Nanowire	11
2.3 BAND THEORY OF SOLIDS	12
2.3.1 Band Structure of Solids	12
2.3.2 Bands for Doped Semiconductors	14
3.0 RESEARCH DESCRIPTION.....	16
3.1 HYPOTHESIS	16
3.2 OBJECTIVES	16

3.3	TASKS	17
4.0	EXPERIMENTAL DETAILS	18
4.1	TIN DIOXIDE NANOWIRE SYNTHESIS	18
4.1.1	The Experimental Process of Nanowire Growth	18
4.1.2	The Mechanism of Nanowire Growth	20
4.2	SUPERCAPACITOR FABRICATION.....	21
4.2.1	Preparation of Electrolyte.....	21
4.2.2	Electrochemical Deposited Manganese/Manganese-nickel Oxide Films..	21
4.3	CYCLIC VOLTAMMETRY	24
4.4	ULTRAVIOLET-VISIBLE SPECTROSCOPE.....	25
4.5	FOUR PROBE CONDUCTIVITY MEASUEREMENT.....	26
4.5.1	Apparatus	26
4.5.2	Theory.....	27
4.6	SCANNING ELECTRON MICROSCOPE	28
5.0	RESULTS AND DISSCUSSION	30
5.1	NANOWIRE GROWTH ON FTO SUBSTRATES	30
5.1.1	Nanowire Morphology	30
5.1.2	The Influence of Sb Doping and Coated Au Thickness on The Sheet Resistance.....	34
5.1.3	The Influence on Optical Properties	35
5.1.4	Discussion about the Impact of Sb on Nanowire Morphology	37
5.1.5	Impact of Sb Doping on Electrical/optical Properties of Nanowires	37
5.1.6	The Impact of Coated Gold on FTO Substrates.....	39
5.2	NANOWIRE BASED SUPERCAPACITOR.....	40

5.2.1	The Influence of the Supercapacitors	40
5.2.2	The Nanostructure of the Capacitors	41
5.2.3	The Possible Mechanism	44
5.2.4	Electrical Behavior Characterization	45
5.2.5	The Influence of Deposition Scan Rate.....	46
5.2.6	The Influence of Mn/Ni Oxide Ratio.....	47
5.2.7	The Results of Different Measuring Scan Rate.....	48
5.3	NANOWIRE GROWN ON MESH.....	50
6.0	CONCLUSION.....	52
	REFERENCES.....	54

LIST OF TABLES

Table 2.1. Optical and electrical properties of ITO summary	8
Table 4.1 SnO ₂ nanowire growth condition.....	19
Table 4.2. Deposition condition.....	23

LIST OF FIGURES

Figure 2.1. EDLC structure [39]	5
Figure 2.2. Pseudocapacitor structure [41]	6
Figure 2.3. The band gap of In_2O_3 and Sn doped In_2O_3 [35].....	9
Figure 2.4. Crystal structure of SnO_2 [38]	10
Figure 2.5. Band structure of insulators, semiconductors and conductors	13
Figure 2.6. Band structure of n-type and p-type semiconductors	14
Figure 4.1. Schematic illustration of growth mechanism	20
Figure 4.2. Three electrodes system [44].....	22
Figure 4.3. Cyclic voltammetry potential waveform [22]	25
Figure 4.4. Four probe apparatus [43]	26
Figure 4.5. Four probe conductivity measurement [43]	27
Figure 5.1. (a) Cross-section view of SnO_2 nanowire; (b) Top view of SnO_2 nanowire; (c) Cross-section view of Sb-doped SnO_2 nanowire; (d) Top view of Sb-doped SnO_2 nanowire	31
Figure 5.2. XRD image of Sb-doped SnO_2 nanowire.....	32
Figure 5.3 The effect of Sb doping	33
Figure 5.4 The effect of the coated Au thickness	33
Figure 5.5 The influence of Sb doping on sheet resistance	34
Figure 5.6 The influence of Au thickness on sheet resistance.....	35

Figure 5.7. The influence of Sb doping on transmission	36
Figure 5.8. The influence of coated Au on transmission	36
Figure 5.9. Sb concentration within SnO ₂ nanowires by EDS when varying dopant concentration	38
Figure 5.10. Au particles on different thickness gold layers	39
Figure 5.11. Ideal core-shell structure	40
Figure 5.12. (a) nanostructure of manganese oxide with voltage 0-1 V; (b) nanostructure of manganese oxide with voltage range 0.4-1.2 V; (c) manganese oxide deposited on FTO.....	41
Figure 5.13. Deposited layer on short nanowires	42
Figure 5.14. Concentration of low voltage range	43
Figure 5.15. Concentration of high voltage range	44
Figure 5.16. CV curves and specific capacitance under different deposition scan rates	46
Figure 5.17. CV curves and specific capacitance of different NiO content samples.....	47
Figure 5.18. CV curves of various measuring scan rates.....	48
Figure 5.19. Specific capacitances under different scan rates	49
Figure 5.20. Nanowire grown on (a) pure SS mesh; (b) gold coated SS mesh	50
Figure 5.21. (a) The lengths of nanowires grown on mesh; (b) The diameters of nanowires grown on mesh	51

ACKNOWLEDGMENT

I would like to express my greatest appreciation to all the people who help me finish this master thesis. I need to show my sincere gratitude to my advisor Prof. Jung-Kun Lee for his motivation and patience. I cannot complete this thesis without his guidance.

In addition, I want to thank those kind members in our group: Dr. Gill-Sang Han, Salim Caliskan, Fangda Yu, Fen Qin, Matthew Lawrence Duff for helping me and sharing their experience with me.

1.0 INTRODUCTION

Transparent conducting oxides, abbreviated as TCOs, are a kind of materials which can offer both high electrical conductance and high optical transmissivity. A limited number of oxide materials possess these two properties simultaneously. It's well known that most transparent materials such as silicon glass are electrical insulators. On the other hand, most semiconductor materials with good electrical conductance such as silicon are wavelength dependent optical resistors. Due to unique physical properties, TCOs are widely used in optoelectrical and photovoltaic devices. Common TCO materials are donor-doped oxides such as SnO_2 , In_2O_3 , ZnO , and their ternary alloys, with tin doped indium oxide (ITO) being the most widely used TCO material. [1] However, the supply of ITO is not stable because of the high cost of indium, so some other low-cost TCO materials are expected to be supplied. As a result, low-cost SnO_2 based TCO materials have attracted a large amount of attention and they are expected to be used in large scale applications for solar cells and light emitting diodes and solar cells. The performance of devices using TCOs may be further improved by using one-dimensional nanostructures. [1]

SnO_2 nanostructure is a classical n-type semiconductor material because of its wide bandgap ($E_g=3.6$ eV, 300k). Doping SnO_2 with cations (e.g. Sb^{5+}) and anions (e.g. F^-) can improve the electrical and optical properties of SnO_2 . It's reported that antimony-doped SnO_2

have high electric conductivity, since electrons are produced to compensate positive charge of Sb in Sn site. Resistivity of SnO₂: Sb thin films can be lower than 10⁻³ Ω cm.

Supercapacitors (or called electrical capacitors) are getting more important because of its ability for fast charging and discharging. When an electrical field is applied, supercapacitors store electric energy through two different mechanisms. In an electrical double-layer capacitor, ions that are accumulated on the surface of electrodes are responsible for the energy storage. In a pseudo-capacitor, both Faraday reaction and double layer formation contribute to the energy storage. In order to increase the electrical capacitors' energy densities, several transition metal oxides are used to offer high capacitance. On their surface, reversible redox reactions occur and a change in a valence state of transition metals increase the charge storage capacity. Several metal oxides, such as MnO₂, NiO, and Fe₃O₄, have been proposed as promising electrode materials because of their environment compatibility, low cost, abundant availability and wide potential windows. [4] MnO₂ is a potential alternative electrode material for ECs and has been broadly studied as a cathode material for batteries. NiO is another promising material because it exhibits good electrochemical stability.

In this study, the doping behavior of Sb into SnO₂ nanowires is first studied. Since the synthesis technique of nanowires is different from that of thin films, the effect of the synthesis method on cation doping needs to be examined. During the growth of thermal vapor deposition, a content of Sb in a melting pool is controlled and composition of melts and nanowires are compared. In addition, different Au thickness coated FTO substrates were also used to grow the nanowires to check the influence of the gold layer because the gold layer catalyzes a nucleation of SnO₂. The morphology and electrical properties of the fabricated nanowires were later characterized to see the impact of antimony dopant and coated gold. In the next step, these thin

nanowire layers are used as substrates for coating of transition metal oxide (manganese oxide and nickel oxide) and the effect of a coating layer composition and a nanowire resistivity on a charge store capability is investigated for an application of supercapacitors. When MnO_2 and NiO are deposited on SnO_2 nanowires, a core-shell structure is expected to form on the nanowires. This device is meaningful because it combines the advantage of SnO_2 nanowires (high conductivity) and manganese oxide and nickel oxide (pseudo-capacitor function). This means the device can have good electrical conductivity and charge storage at the same time.

In addition, Stainless steel (SS) mesh was also used as substrates to grow SnO_2 nanowires because it has two dimensions which is different from FTO substrates. Nanowires grown on pure SS mesh and Au coated SS mesh are compared to study the influence of a gold layer. It has also been found that the growing temperature may also have an impact on the structure and properties of the nanowires grown on SS mesh.

2.0 BACKGROUND INFORMATION AND LITERATURE REVIEW

This chapter is to introduce some knowledge about supercapacitors and SnO₂ nanowires. Additionally, several necessary electrical and optical properties are introduced as well.

2.1 SUPERCAPACITOR

A supercapacitor is an electrochemical capacitor with high-capacity. Its capacitance is much higher than that of electrical capacitor. Typically, supercapacitors can store 100 times energy more than electrolytic capacitors. Compared with conventional capacitors, supercapacitors use electrostatic double-layer capacitance or electrochemical pseudocapacitance or a combination of both.

2.1.1 Electrostatic Double-layer Capacitors (EDLC)

Electrostatic double-layer capacitors store the energy by double layer effect. The electrolyte ions are separated by an inner Helmholtz plane and it can be seen from figure 2.1 that cations accumulate and form a double layer structure with negative electrode, meanwhile, anions accumulate and form a double layer structure with positive electrode. So, the conductor

electrodes and electrolyte ions can perform like a physical capacitor to storage energy. A EDLC can charge and discharge more than 1 million times because there is no limitation of charge transfer kinetics like batteries.

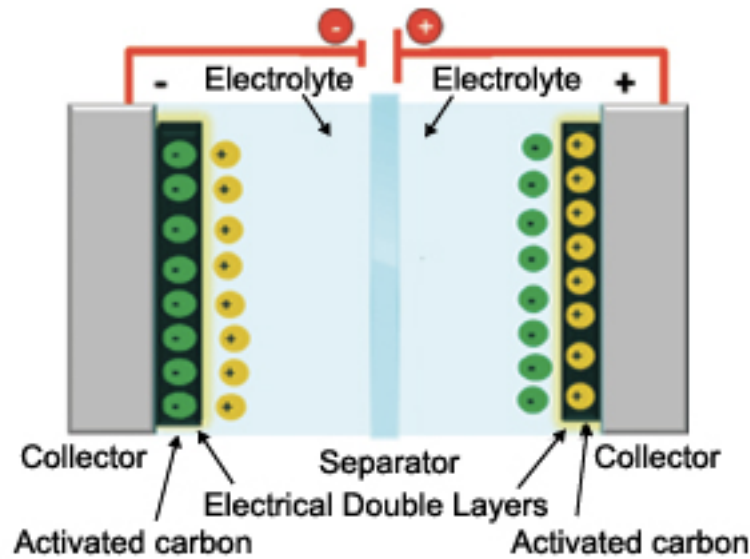


Figure 2.1. EDLC structure [39]

2.1.2 Pseudocapacitors

Pseudocapacitors can store energy through redox reactions and intercalation processes to complete the transfer of charges between electrodes and electrolyte. A pseudocapacitor can store 100 times energy as large as a double-layer capacitor with the same surface can. It has been stated above that there are no chemical reactions in the electrodes during the energy storage process of an electrostatic double-layer capacitor. However, a pseudocapacitor has chemical reactions in the electrodes with an interaction between the ions and the electrodes. In other words, there is an electron charge transfer between the electrode and the electrolyte. Varying

from batteries where the transfer ions cling to the atomic structure of the electrodes, pseudocapacitors store the faradic energy with fast redox reactions. That's the reason why pseudocapacitors can have a much faster charge and discharge speed than batteries. Pseudocapacitors always use conductive polymer or metal oxide as electrodes with a high amount of pseudocapacitance. Figure 2.2 shows the structure of a pseudocapacitor.

Pseudocapacitance with specifically adsorbed ions

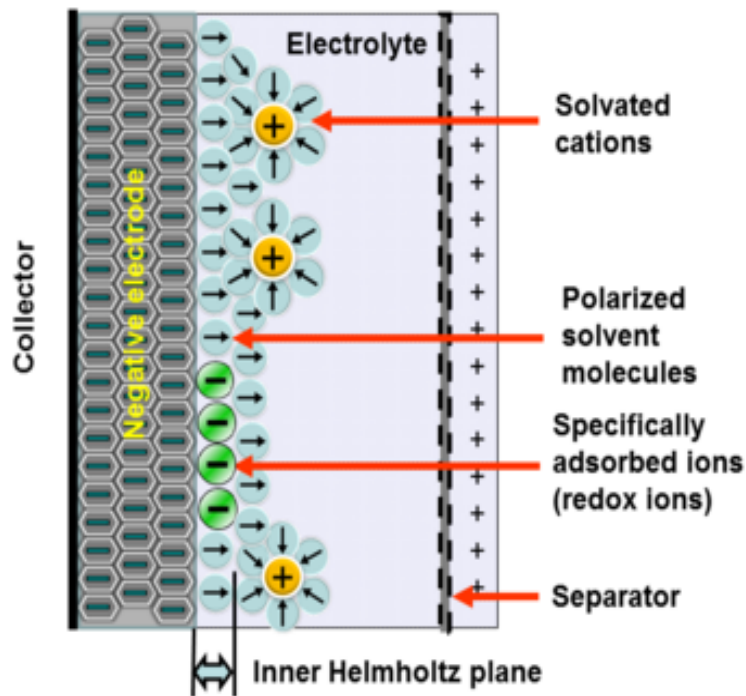


Figure 2.2. Pseudocapacitor structure [41]

2.2 TRANSPARENT AND CONDUCTING OXIDES

Transparent conducting oxides (TCO) are electrical conductive and optical transparent thin film materials. They are widely used to fabricate optoelectronic devices such as solar cell, photovoltaics and OLEDs. In this chapter, a literature review of TCOs is introduced.

2.2.1 TCOs Development

The optical transparency and electrical conductivity depend on the band gap of the material. In metallic materials, a high density of free electrons sit upper the fermi energy, which leave the transmission caused by the reaction with low energy photos. This is the reason why metals always show a high electrical conductivity but low transmittance. Additionally, in most insulate materials, valence band and conductive band are separated by the band gap, which enable the transmission for different wavelength lower than the band gap. That is why insulate materials always have high transparency. More interests are attracted by transparent conducting oxides (TCO) because they can compromise both these two advantages.

A TCO is a wide band-gap semiconductor that has a relatively high concentration of free electrons in its conduction band. These arise either from defects in the material or from extrinsic dopants, the impurity levels of which lie near the conduction band edge. [37] The high concentration of electron carrier (the materials are assumed to be n-type semiconductors) leads to absorb the electromagnetic radiation in both infrared and visible portions of the spectrum.

2.2.2 Indium tin oxide (ITO)

Indium tin oxide (ITO) is composed of indium, tin and oxygen in different proportions. The typical composition of these three elements are 74% In, 8% Sn and 18% O₂ by weight. ITO has been regarded as one of the most important conductive transparent oxides these years because of its electrical conductivity and optical transparency. Indium tin oxide has been used to fabricate many applications nowadays such as polymer-based electronics, smart windows and flat-panel displays. ITO can be synthesized via deposition method and different method may lead to different properties of the produced ITO. Table 2.1 lists different ITO produced by different techniques and their properties.

Table 2.1. Optical and electrical properties of ITO summary

Deposition technique	Thickness (nm)	Hall mobility $\mu\text{H (sm}^2\text{V}^{-1}\text{s}^{-1}\text{)}$	Carrier concentration (cm ⁻³)	Resistivity (Ωcm)	Transmittance (%)
r.f. sputtering	700	35	6×10^{20}	3×10^{-4}	90
r.f. sputtering	500	12	12×10^{20}	4×10^{-4}	95
r.f.sputtering	400	25	3×10^{20}	8×10^{-4}	-
Magnetron sputtering	800	26	6×10^{20}	4×10^{-4}	85
d.c sputtering	100	35	9×10^{20}	2×10^{-4}	85
Reactive evaporation	250	30	5×10^{20}	4×10^{-4}	91
Ion beam sputtering	60	26	2×10^{20}	12×10^{-4}	-

It can be seen from the table that the best ITO shows the lowest resistivity which is as low as $2 \times 10^{-4} \Omega \text{cm}$. At the same time, its transmission is also high: 85%. The combination of optical and electrical properties is the judgment criteria of the quality of a ITO. The mobility is enhanced because the crystallinity of thin films using higher temperature. And the band gaps of ITO range from 3.5eV to 4.06eV, which is wider than the visible radiation and is the reason of high transparency of ITOs. [34] The carrier concentration will increase with Sn dopant and the absorption limit will shift from the ultraviolet radiation area into shorter wavelength area. The band gap of In_2O_3 and Sn doped In_2O_3 is shown in Figure 2.3. It can be seen that the Fermi level has jumped into conduction band after Sn doping, which increase the optical band gap.

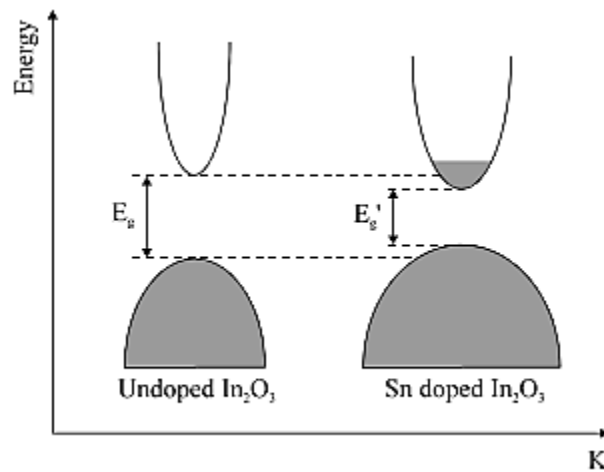


Figure 2.3. The band gap of In_2O_3 and Sn doped In_2O_3 [35]

2.2.3 Tin Dioxide

Tin dioxide is the compound with the chemical formula SnO_2 . The mineral form of tin dioxide is known as cassiterite. Its crystal structure is shown in figure 2.4, which shows that each tin atom

is 6 coordinate and each oxygen atom is 3 coordinate. It has been reported that Tin dioxide is an important metal oxide material for a range of electrical applications. For example, SnO₂ is always used to fabricate conductance-type gas sensors because the electrical conductivity of tin dioxide depends on its surface properties, as molecular absorption or desorption can affect the space-charge layer and the band modulation. In addition, it has been proven that tin dioxide with appropriate dopants (such as Ta, F, and Sb) has potential to play a significant role in the modern devices. For example, doped SnO₂ is always applied as transparent conductive oxide (TCO) materials because of their high conductivity and large bandgap (3.6eV). SnO₂ based TCO films are expected to be a low-coat alternative to indium tin oxide films in various optoelectronic devices, such as flat-panel displays, solar cells, and light-emitting diodes. [3] Some other studies found that Co or Ni doped SnO₂ can perform as a magnetic semiconductor and exhibit Curie temperature. As the advantages of the nanostructure, SnO₂ nanowires/nanobelts have attracted a lot of attention. In general, tin oxide is a popular n-type semiconductor oxide with wide band gap (3.6eV).

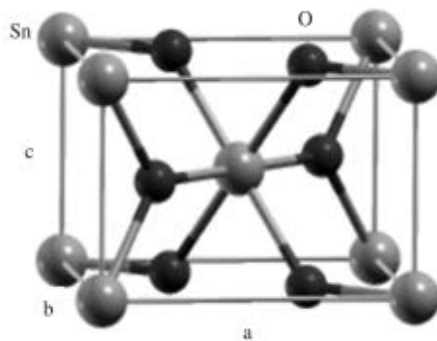


Figure 2.4. Crystal structure of SnO₂ [38]

2.2.4 Vapor Liquid Solid (VLS) Method for Nanowire Growth

VLS (Vapor-liquid-solid) method is a common technique to synthesize the nanowires. The advantage of this method is the nanowires synthesized via this technique have high quality and density. To make this method be more efficient, the catalyst is always required. Liquid metal nanoclusters are regarded as the best choices to be the catalyst such as gold (Au). Growing Si nanowires can be used as an example. When the gold nanoparticles are present on the growth substrate, the VLS process proceeds in three main steps. Firstly, the alloying process consists of the formation of liquid droplet containing the metal catalyst and dissolved Si. For gold, the eutectic composition is obtained at 363 °C. Secondly, when the silicon concentration reaches the upper solubility limit, nanowire nucleation commences. At this stage, a three phases biphasic system (SiH₄ gas, Au/Si alloy and Si solid) may be attained, the Au/Si liquid droplet being intercalated between the gaseous and the solid phases. Thirdly, the axial growth arising from further dissolution of Si into the liquid phase and simultaneous crystal packing at the bottom leads to a forward push of the catalytic phase to form a nanowire. On completion of the nanowire growth phase, the gold catalyst is observed at the nanowire tips. [24]

2.2.5 Sb Doped SnO₂ Nanowire

More and more studies were focused on the doping materials for tin dioxide because the intrinsic SnO₂ nanowires exhibit high resistivity and low carrier concentration. The electrical and optical properties of SnO₂ nanowires can be modulated by doping with appropriate materials. One of the most promising doping mat

erials of is antimony (Sb) due to its facility of incorporation in the SnO₂ lattice leading to measurable improvements in electrical conductivity and optical transparency. [27] It is expected that Sb doped SnO₂ nanowires may provide an inexpensive alternative to ITO as transparent conducting oxide materials. [1] Till now, single crystalline transparent conducting Sb-doped tin oxide nanowires are successfully synthesized by various methods. A lot of electrical transparent characterizations have demonstrated that the antimony doped SnO₂ nanowires are metallic conductors with very low resistivity. Wan et al. reported that the antimony doped tin dioxide nanowires can have a resistivity around 10^{-4} Ωcm and failure current densities up to 10^7 A/cm². These reports show that the ATO nanowires could be provided as inexpensive TCO materials to be regarded as alternatives to ITO.

2.3 BAND THEORY OF SOLIDS

2.3.1 Band Structure of Solids

The difference between conductors, semiconductors and insulators can be visualized by plotting the available energy for electrons in the material. Differing from free atoms who have discrete energies, the available energies state form bands. Crucial to the conduction process is whether or not there are electrons in the conduction band. [13] The electrons in insulators in the valence band are separated from the conduction band by a large band gap. However, in conductors the conduction bands overlap the valence bands, and in semiconductors there are small enough band gaps between the conduction and valence bands that several diverse kinds of excitations can

bridge the gaps. Due to the small band gaps, some doping materials can increase conductivity of semiconductors.

Fermi level is an important parameter in the band theory of solids. Fermi level is used to be regarded as the hypothetical energy level of electrons which would have a fifty percent probability to be occupied. In this way, the position of the fermi level is crucial in determining electrical properties. Figure 2.5 shows the energy band structure of insulators, semiconductors and conductors. It can be clearly understood from this figure that no electrons from the valence band can reach the conduction band because of the large band gap between the conduction and valence bands in insulators. Meanwhile, in semiconductors, the band gap is not so large that some excitation such as thermal energy can bridge the band gap for a fraction of electrons. And in conductors, there is no gap since the two bands are overlapped.

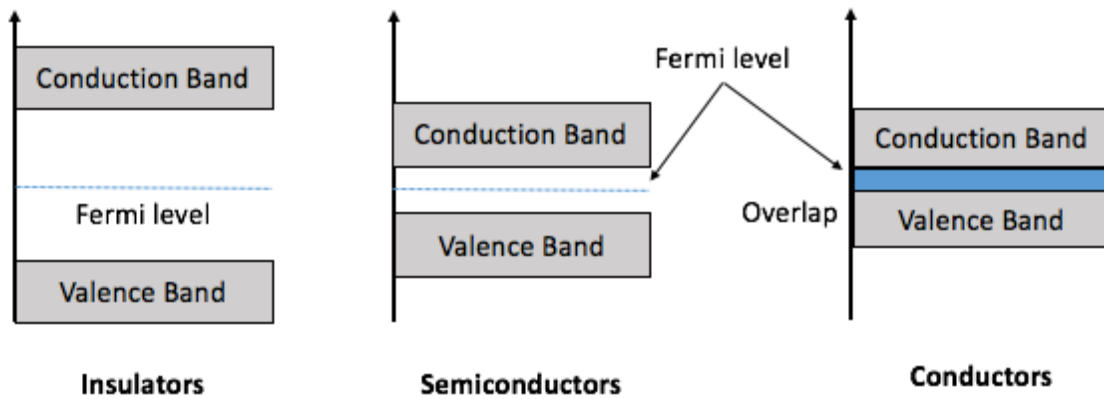


Figure 2.5. Band structure of insulators, semiconductors and conductors

The band structure of semiconductors is always more noteworthy because of its wide use. For intrinsic semiconductors such as germanium and silicon, the fermi level is halfway between the conduction and valence bands. When the temperature is increased, a few electrons can reach

the conduction band to provide some current. For extrinsic semiconductors such as p-type or n-type semiconductors, extra energy levels are added.

2.3.2 Bands for Doped Semiconductors

The band theory of doped semiconductors shows extra levels are added by the impurity. In n-type semiconductors there are extra electron energy levels near the bottom of the conduction band so that these electrons can be easily excited to reach the conduction band. In p-type semiconductors, extra holes' energy levels are near the top of valence band so that the electrons in the valence band are easily to be excited to leave mobile holes in the valence band. Figure 2.6 shows the band structure of n-type and p-type semiconductors.

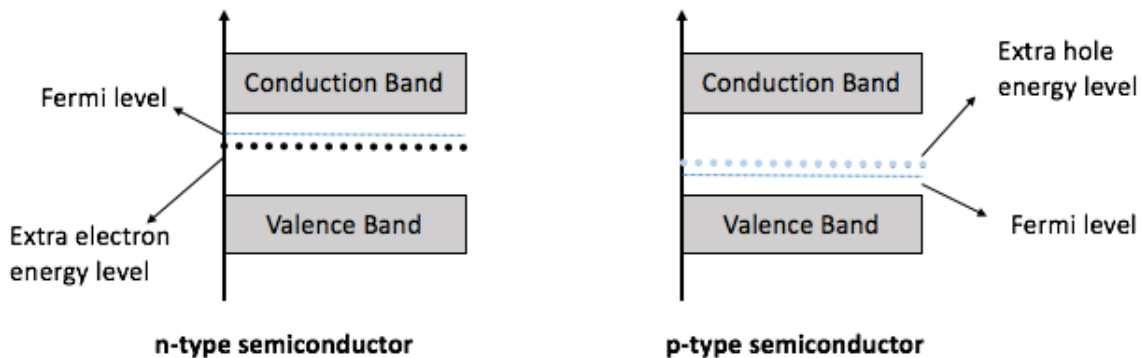


Figure 2.6. Band structure of n-type and p-type semiconductors

For n-type semiconductors, the electrons are regarded as the majority carriers for current flow and donors provide more electrons. On the contrary, for p-type semiconductors, the holes are regarded as the majority carriers for current flow and donors provide more holes.

In this thesis, SnO₂ is n-type semiconductor and antimony are doped to provide more free electrons to increase the electrical conductivity.

3.0 RESEARCH DESCRIPTION

3.1 HYPOTHESIS

The hypothesis of this study is that the doped antimony can affect the morphology of tin oxide nanowires and improve the optical and electrical properties of the nanowires. Another hypothesis of the study is that the electrical properties of manganese oxide-nickel oxide capacitors are better than intrinsic manganese oxide capacitors under the same conditions.

3.2 OBJECTIVES

A main goal of this research is to study the electrical properties of intrinsic and Sb doped SnO₂ nanowires grown on FTO substrates and their application to supercapacitors. The role of pure manganese oxide and manganese oxide-nickel oxide mixture on a charge storage capability is discussed. In addition, the stainless-steel mesh is used as the substrates for SnO₂ nanowire growth and the effect of two substrates (stainless-steel mesh and FTO glass) is compared.

3.3 TASKS

The first task of this research is to fabricate the intrinsic SnO₂ nanowires and Sb doped SnO₂ nanowires on FTO substrates using VLS method and study the morphology and properties of the nanowires grown at different conditions. The second task is to study the morphology of the nanowires grown on stainless-steel mesh and compare the effect of substrates on the nanowire growth. The third task focuses on fabricating the supercapacitors by coating a manganese oxide layer or a manganese oxide – nickel oxide mixture layer on the surface of nanowires. Electrochemical properties of intrinsic manganese oxide and manganese oxide – nickel oxide mixture is measured to examine the role of Ni in a pseudocapacitive reaction.

4.0 EXPERIMENTAL DETAILS

4.1 TIN DIOXIDE NANOWIRE SYNTHESIS

4.1.1 The Experimental Process of Nanowire Growth

In this thesis, tin oxide nanowires are synthesized via VLS (vapor-liquid-solid) method. A quartz tube furnace was used to synthesize the nanowire array. Fluorine tin doped oxide (FTO) was used as the substrates to grow the nanowires. Before the synthesis, a thin gold (Au) layer was deposited onto the surfaces of the FTO substrates by e-beam. Three different thicknesses (1.5nm, 3nm and 6nm) of gold layer were used to cause the solidification of Sn and Sb from a gas state. Different thicknesses were used to change the morphology and density of nanowires. High purity (99.99%) tin and antimony were used as the metal sources for thermal evaporation. Three different weight ratios of Sn-Sb mixtures were tested to change (Sn: Sb=100: 5, 100: 10 and 100: 15) the content of Sb in SnO₂ nanowire. A metal powder source was positioned on a quartz boat and then this quartz boat was inserted into a horizontal tube furnace. Six Au/FTO substrates were also placed into the tube furnace and a distance between a closer end of the quartz boat and a nearest substrate was 6mm. A inside of the tube was evacuated first to reach base pressure of 1mTorr. Then argon flowed rate of 50 sccm (Ar, purity: 99%) and pressure inside a tube was maintained at 1 Torr. The furnace was heated from the room temperature to 800 °C at a rate of 10

$^{\circ}\text{C min}^{-1}$. Once the temperature was stabilized at 800°C , the oxygen gas was introduced into the tube to grow oxide nanowires. After 20 minutes long nanowire growth, the furnace was cooled naturally. Table 4.1 shows the growth condition of the nanowires.

Table 4.1 SnO₂ nanowire growth condition

Condition Number	Growth Time (min)	Growth Temperature ($^{\circ}\text{C}$)	Gold Thickness (nm)	Weight Ratio Of Sb: Sn (%)	Substrates
1	20	800	1.5	0	FTO
2	20	800	1.5	2.5	FTO
3	20	800	1.5	5	FTO
4	20	800	1.5	10	FTO
5	20	800	1.5	15	FTO
6	20	800	3	0	FTO
7	20	800	6	0	FTO
8	20	800	3	5	FTO
9	20	800	3	10	FTO
10	20	800	3	15	FTO
11	20	800	6	5	FTO
12	20	800	6	10	FTO
13	20	800	6	15	FTO

The growth conditions of the nanowires are listed in Table 4.1 above, including growth time, growth temperature, thickness of a gold layer, a weight ratio of Sb: Sn and the substrate

types. FTO and stainless steel mesh were used as the substrates for the nanowire growth. These nanowire samples were divided into three groups for different purposes. The samples of the first group were used to check the morphology of the nanowires via scanning electron microscope (SEM). The samples of the second group were used to check the electrical properties of the nanowire. The samples of the third group were used as the substrate to fabricate the supercapacitors.

4.1.2 The Mechanism of Nanowire Growth

During the reaction process, the coated gold plays the role as catalysts. The gaseous tin after annealing and oxygen can form a small globule with gold at the tip of the nanowire. This liquid alloy droplet may have a low freezing temperature. And when the SnO_2 from the droplet starts to precipitate, the nanowire starts to grow. The schematic illustration of this process was shown in Fig 4.1.

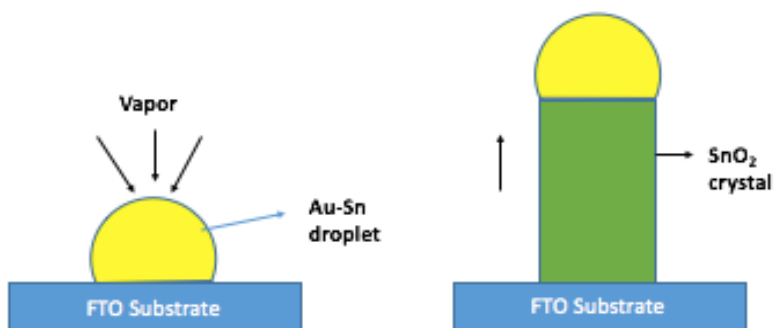


Figure 4.1. Schematic illustration of growth mechanism

4.2 SUPERCAPACITOR FABRICATION

4.2.1 Preparation of Electrolyte

Transition metal oxide layers were coated on nanowires via electrochemical deposition. The first step of this operation was to make the electrolyte. In this thesis, 15mL of 0.05 M manganese acetate tetrahydrate, $\text{Mn}(\text{CH}_3\text{COO})_2 \cdot 4\text{H}_2\text{O}$, 15mL of 0.25 M nickel acetate tetrahydrate, $\text{Ni}(\text{CH}_3\text{COO})_2 \cdot 4\text{H}_2\text{O}$, were mixed to fabricate the electrolyte. According to several reports, the best PH value for this deposition is 6. In this way, PH value of the solution was controlled at 6 by sulfuric acid, H_2SO_4 , at all time.

4.2.2 Electrochemical Deposited Manganese/Manganese-nickel Oxide Films

Manganese and manganese-nickel oxide thin films were deposited on the substrates via three electrodes method, as shown in figure 4.2. The electrolyte was intrinsic $\text{Mn}(\text{CH}_3\text{COO})_2 \cdot 4\text{H}_2\text{O}$ or the mixture of $\text{Mn}(\text{CH}_3\text{COO})_2 \cdot 4\text{H}_2\text{O}$ and $\text{Ni}(\text{CH}_3\text{COO})_2 \cdot 4\text{H}_2\text{O}$. The three electrodes system consists of three electrodes: the working electrode, the reference electrode and the counter electrode. In this thesis, the SnO_2 nanowire grown on the FTO substrates were used as the working electrode. A platinum (Pt) sheet was used as the counter electrode and Ag/AgCl was used as the reference electrode. The electrodeposition mode in this thesis was potentiodynamic (cyclic voltammetry [CV]). After the deposition, Manganese and manganese-nickel oxide coated nanowires were annealed at 300 °C in air for 6 hours.

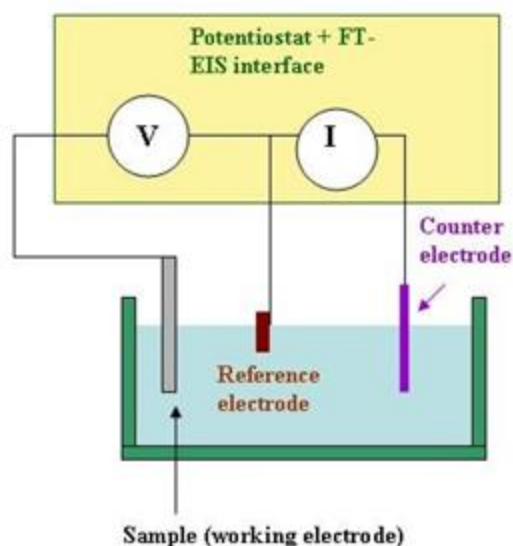


Figure 4.2. Three electrodes system [44]

Table 4.2 lists the parameters of the electrochemical deposition. During the deposition process, several parameters were considered to affect the properties of the fabricated supercapacitors: the ratio of $\text{Mn}(\text{CH}_3\text{COO})_2 \cdot 4\text{H}_2\text{O}$ and $\text{Ni}(\text{CH}_3\text{COO})_2 \cdot 4\text{H}_2\text{O}$ in the electrolyte; the working potential and the deposition scan rate. Four different ratios of $\text{Mn}(\text{CH}_3\text{COO})_2 \cdot 4\text{H}_2\text{O}$ and $\text{Ni}(\text{CH}_3\text{COO})_2 \cdot 4\text{H}_2\text{O}$ were used in the experiment: 1:0; 1:1; 1:3 and 1:5. Then two working potentials were tried to process the deposition: 0-1 V and 0.4-1.2V. In addition, three different deposition scan rates were used during the deposition: 10 mVs^{-1} ; 15 mVs^{-1} and 20 mVs^{-1} . These parameters were proved to have an influence on the fabricated pseudocapacitors in the following testing experiments.

Table 4.2. Deposition condition

Condition Number	Substrates	Electrolyte Ratio of Mn/Ni	Working Potential (V)	Scan Rate (mVs ⁻¹)	Deposition Cycle
1	Pure SnO ₂ nanowire	1:0	0-1	20	7
2	Pure SnO ₂ nanowire	1:0	0.4-1.2	20	7
3	Pure SnO ₂ nanowire	1:1	0.4-1.2	20	7
4	Pure SnO ₂ nanowire	1:3	0.4-1.2	20	7
5	Pure SnO ₂ nanowire	1:5	0.4-1.2	20	7
6	Pure SnO ₂ nanowire	1:5	0.4-1.2	15	7
7	Pure SnO ₂ nanowire	1:5	0.4-1.2	10	7
8	5% Sb doped SnO ₂ nanowire	1:5	0.4-1.2	20	7
9	10% Sb doped SnO ₂ nanowire	1:5	0.4-1.2	20	7
10	15% Sb doped SnO ₂ nanowire	1:5	0.4-1.2	20	7

Applied electric field was monitored via three electrodes system as well. The electrolyte is 0.5M sodium sulfate solution. A thin platinum sheet was used as a counter electrode; the deposited samples were used as working electrodes and Ag/AgCl was used as a reference electrode. CV curves were recorded in the voltage window ranging from 0 to 1 V with a scan rate of 20 mV/s. The capacitance of the deposited metal oxide can be calculated by equation 4.1.

$$C = (\int I dt)/(\Delta V \times m) \quad (4.1)$$

Where I is the oxidation current, m is the mass of deposited metal oxide; dt is the time differential and ΔV is the potential.

In addition, the power P and the energy E densities can be calculated by equation 4.2 and 3, respectively:

$$P = V^2/2 \quad (4.2)$$

$$E = (V^2)/(4R_s) \quad (4.3)$$

where V is the potential and R_s is the equivalent resistance of this device.

4.3 CYCLIC VOLTAMMETRY

Cyclic voltammetry (CV) is the electrodeposition mode in this research. CV mode indicates cycling the potential of an electrode. The potential of the working electrode can be controlled by a reference electrode such as a silver/silver chloride electrode (Ag/AgCl). The potential applied

across these two electrodes can be regarded as a signal. This signal is a linear potential scan with a triangular waveform. [36]

The waveform of cyclic voltammetry is shown in figure 4.3. It can be seen from the figure that the cycle is t_2-t_0 , the potential increases linearly over time in the first half of the cycle and decreases linearly over time in the second half.

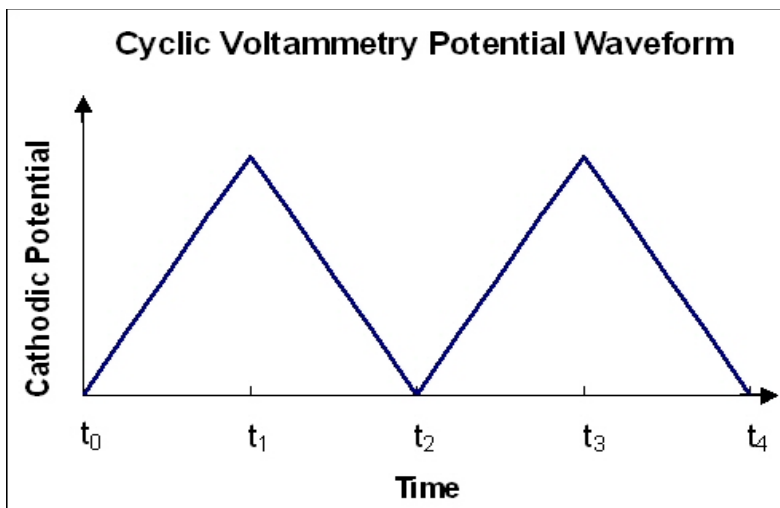


Figure 4.3. Cyclic voltammetry potential waveform [22]

4.4 ULTRAVIOLET-VISIBLE SPECTROSCOPE

Ultraviolet- visible spectrophotometer was used to measure the transmittance and absorbance of the intrinsic and Sb doped SnO_2 nanowires grown on the FTO substrates. Two types of parameters were measured: transmittance and absorbance. We can use I to indicate the intensity of light passing through our samples and I_0 to indicate the intensity of light before passing through our samples. The ratio I/I_0 is the transmittance (%T). The absorbance (A) is based on the transmittance, as shown in equation 4.4.

$$A = -\log\left(\frac{\%T}{100\%}\right) \quad (4.4)$$

4.5 FOUR PROBE CONDUCTIVITY MEASUREMENT

4.5.1 Apparatus

The sheet resistance of the nanowire was measured via four probe method. The experimental apparatus consists of four probes, sample holder, constant current generator, digital panel meter and oven power supply. This four probe method is regarded as one of the most widely used methods to measure the resistivity of semiconductors. Semiconductor materials deposited on substrates can be measured via this way. It can be seen from the following figure 4.4. It consists of four probe arranged linearly in a straight line at equal distance S from each other. A constant current is passed through the two probes and the potential drop V across the middle two probes is measured.

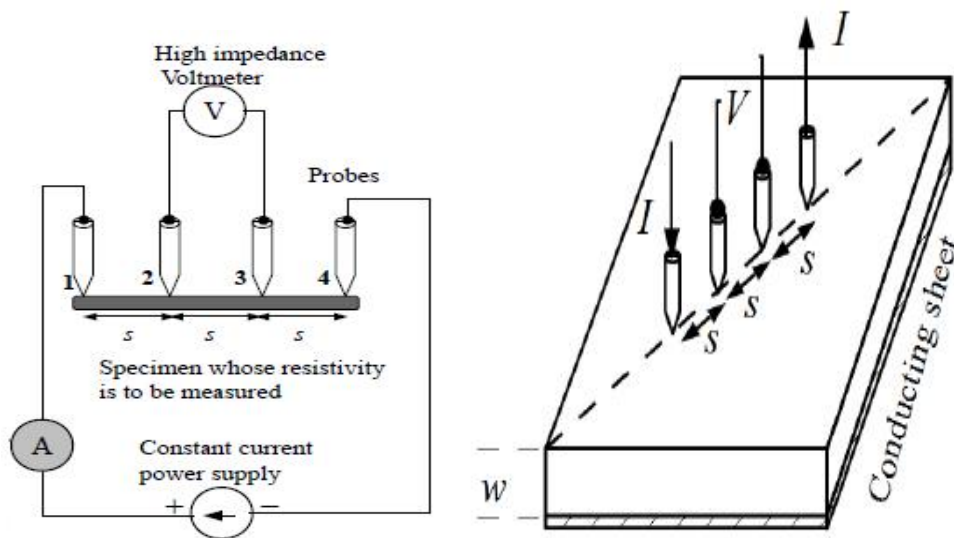


Figure 4.4. Four probe apparatus [43]

The theory of measuring the sheet resistance of tin oxide nanowire via four probe method in this thesis is the relationship between the resistance and the length & cross section area of the semiconductor. At the constant temperature, the resistance (R) is proportional to the length (L) and inversely proportional to the cross section area (A). The relationship can be illustrated as equation 4.5.

$$R = \rho \frac{L}{A} = \rho \frac{L}{Wt} \quad (4.5)$$

$$R = \frac{\rho L}{tW} = R_s \frac{L}{W} \quad (4.6)$$

where ρ is the resistivity ($\Omega \cdot m$), L is the length and A is the cross section area. W and t are width and thickness, respectively. Define sheet resistance (R_s) equals to ρ / t , shown in equation 4.6. Its unit is ohms or ohms per square (Ω / sq).

4.5.2 Theory

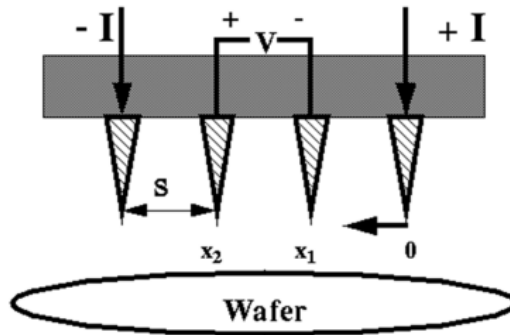


Figure 4.5. Four probe conductivity measurement [43]

Four probe conductivity measurement is shown in figure 4.5. For a film sample with small thickness ($t \ll s$), we have $A = 2\pi xt$. The resistance can be calculated via equation 4.7.

$$R = \int_{x_1}^{x_2} \rho \frac{dx}{2\pi xt} = \int_{1s}^{2s} \rho \frac{dx}{2\pi xt} = \frac{\rho}{2\pi t} (\ln x) \Big|_s^{2s} = \frac{\rho}{2\pi t} \ln 2 \quad (4.7)$$

So the sheet resistivity of the sample can be calculated by equation 4.8:

$$\rho = \frac{\pi t V}{\ln 2 I} \quad (4.8)$$

And sheet resistivity is defined as:

$$R_s = \frac{\rho}{t} = k \left(\frac{V}{I} \right) \quad (4.9)$$

Where k is a geometric factor, which for a semi-infinite thin film is 4.53.

4.6 SCANNING ELECTRON MICROSCOPE

In this thesis, scanning electron microscope (SEM) was used to check the morphology of the tin oxide nanowires grown on FTO substrates and stainless steel mesh. SEM produces images of the samples by scanning the samples with a highly focused beam of electron. These images are always obtained by secondary electrons, which are emitted at the surfaces of the samples. Thus, SEM can get high-resolution images of the samples' surfaces.

Energy-dispersive X-ray spectroscopy (EDX) was also used in this thesis. SEM could provide the EDX to analyze the composition and elemental content of the specimens. EDX analysis relies on the interaction of x-ray excitation source and the sample. Its chemical

characterization is due to the basic principle that each single element has its own unique atomic structure, which lead to a unique peak on the electromagnetic emission spectrum. There are four primary components of the EDX equipment: the excitation source, the X-ray detector, the pulse processor and the analyzer.

5.0 RESULTS AND DISCUSSION

This chapter describes the results of tin oxide nanowires grown on FTO and SS mesh and discusses the influence of different growing factors on the morphology and electrical properties of tin oxide nanowires: the thickness of gold deposited on the FTO substrates, growing with doped antimony with different weight ratio and nanowire grown time. In addition, this chapter also illustrates the electrical properties of the fabricated electrical capacitors. In this thesis, several factors were tested to get the best electrical capacitors such as the different substrates, scan rate of deposition and different ratio between manganese acetate and nickel acetate.

5.1 NANOWIRE GROWTH ON FTO SUBSTRATES

5.1.1 Nanowire Morphology

The growth of tin oxide nanowire was completed via VLS method on FTO and stainless steel mesh. The nanostructure of the nanowire was checked by SEM and the lengths and widths of tin nanowire were observed through SEM images. Figure 5.1 shows the tin oxide nanowire SEM images. It can be seen that the grown nanowire was a little bit tilting. In addition, the Sb doped nanowire is longer and started to bend because of the gravity.

According to the analysis of the result, the doped antimony and different thickness gold coated on FTO substrates have an impact on the morphology and electrical properties of the nanowire. When FTO was used as the substrates, different weight ratio (5%, 10% and 15%) of antimony was added into the growth process. Through the measurement of nanowire of the SEM images, we found that the length and the diameter of the nanowire increased after adding the antimony.

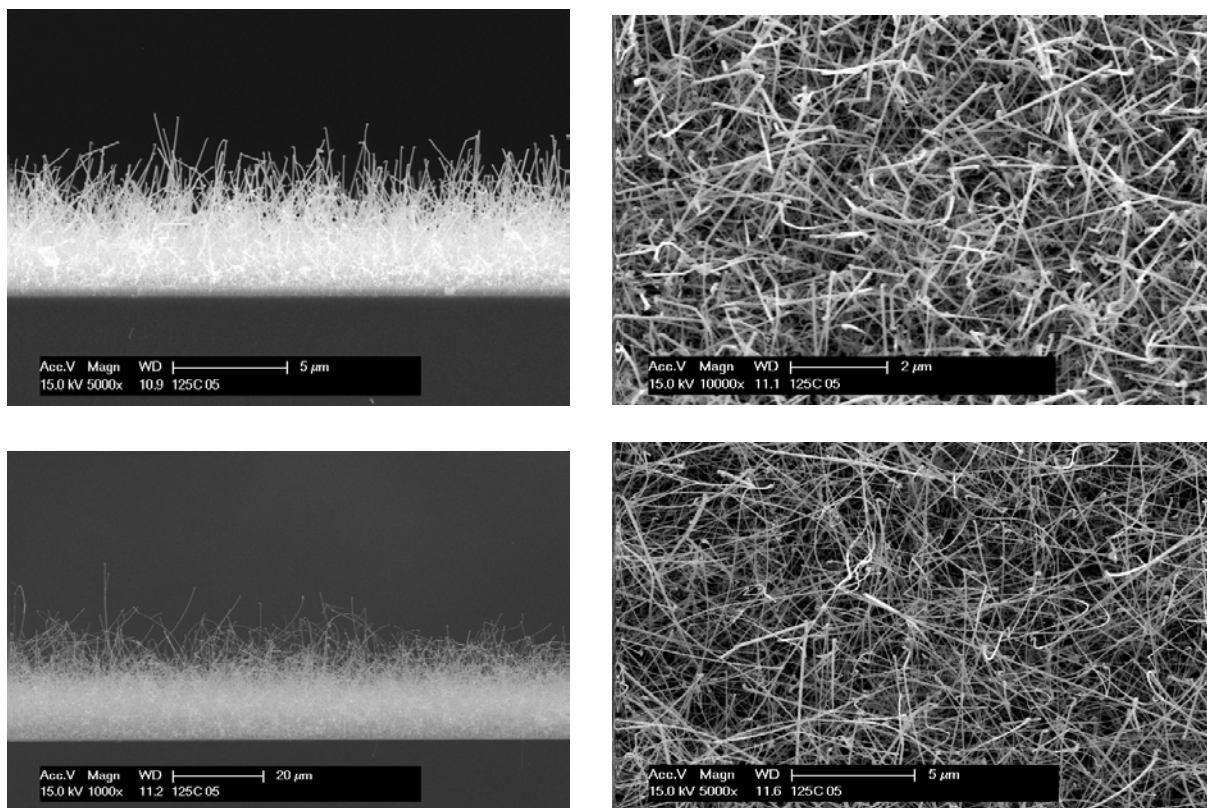


Figure 5.1. (a) Cross-section view of SnO₂ nanowire; (b) Top view of SnO₂ nanowire; (c) Cross-section view of Sb-doped SnO₂ nanowire; (d) Top view of Sb-doped SnO₂ nanowire

Figure 5.2 shows the XRD results of different content Sb doped SnO₂ nanowires. No Sb peaks can be found in the XRD image and it can be assumed that Sb is incorporated into SnO₂ lattice.

After measuring the length and diameter of the nanowire via software ImageJ, we found that the average length of un-doped SnO₂ nanowire is around 15 μm and the average diameter is about 60 nm. However, the doped SnO₂ nanowire has an average length of 20-30 μm and an average diameter of 100 nm. In addition, the coated gold layer with different thickness has an impact on the morphology of the nanowires as well. Three different thickness were used in this thesis: 1.5nm,3nm and 6nm. Figure 5.3 and 5.4 show the influence of Sb doping and coated Au layer thickness on the length and diameter on the SnO₂ nanowire.

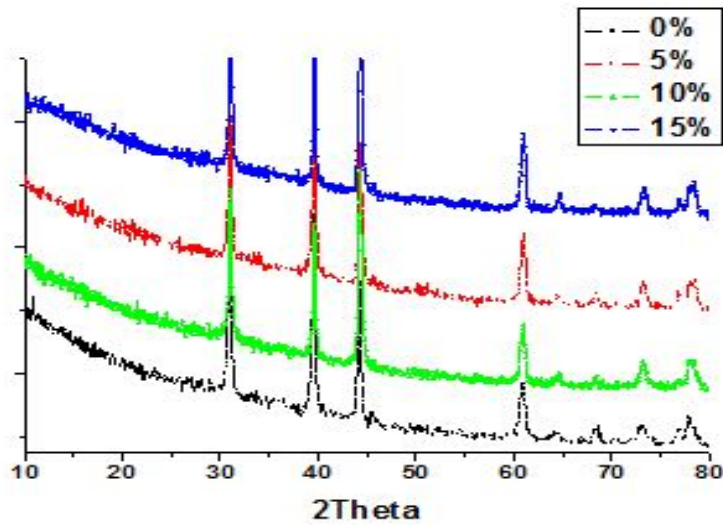


Figure 5.2. XRD image of Sb-doped SnO₂ nanowire

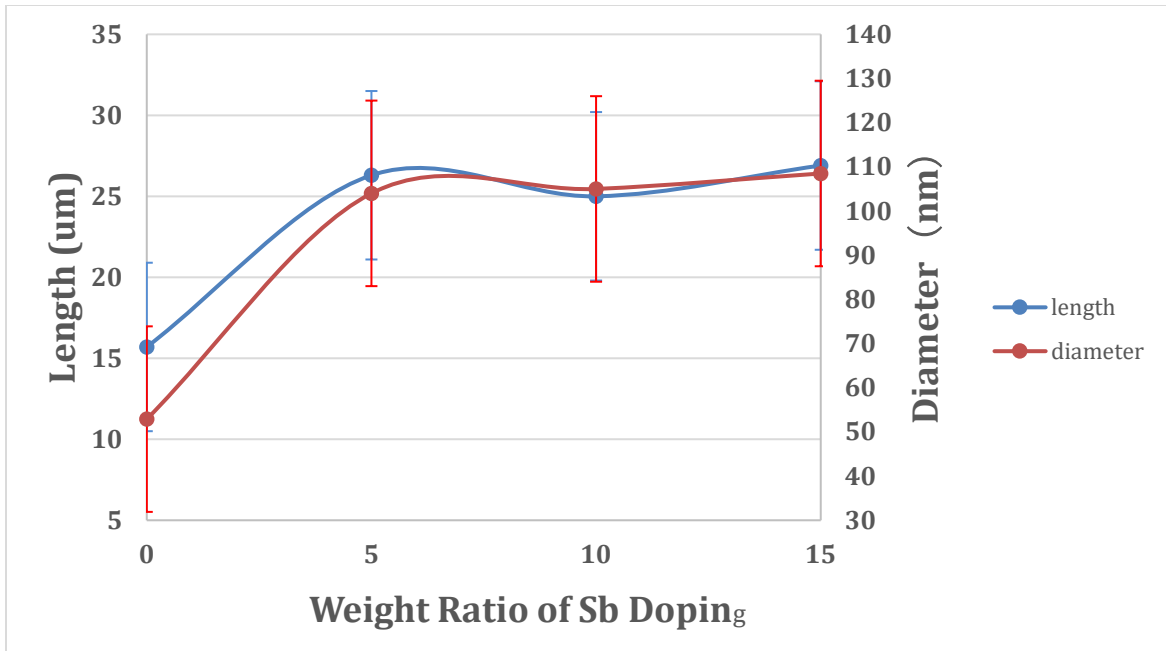


Figure 5.3 The effect of Sb doping

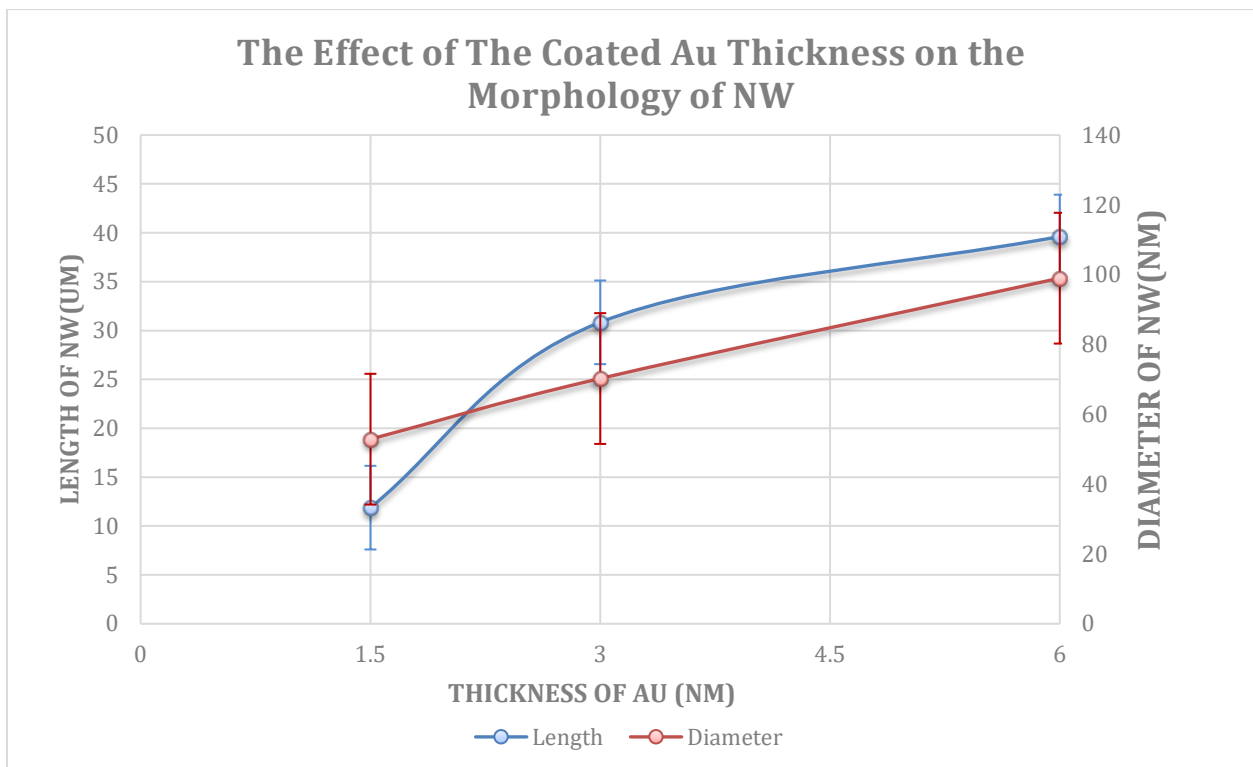


Figure 5.4 The effect of the coated Au thickness

From the testing results, it can be seen that Sb dopant increase both the diameter and length of the nanowires. However, the morphology of nanowires seems not changing when the

doped Sb contents beyond 5%. In addition, the diameter and length are increasing continuously when the thickness of coated gold is increased.

5.1.2 The Influence of Sb Doping and Coated Au Thickness on The Sheet Resistance

The sheet resistance of the SnO₂ nanowire was measured via four points probe. According to the testing results, the doped antimony with different weight ratio and coated gold layer with different thickness can both increase the conductance of nanowire layer. Figure 5.5 and 5.6 exhibit the change of the nanowire sheet resistance due to these two factors.

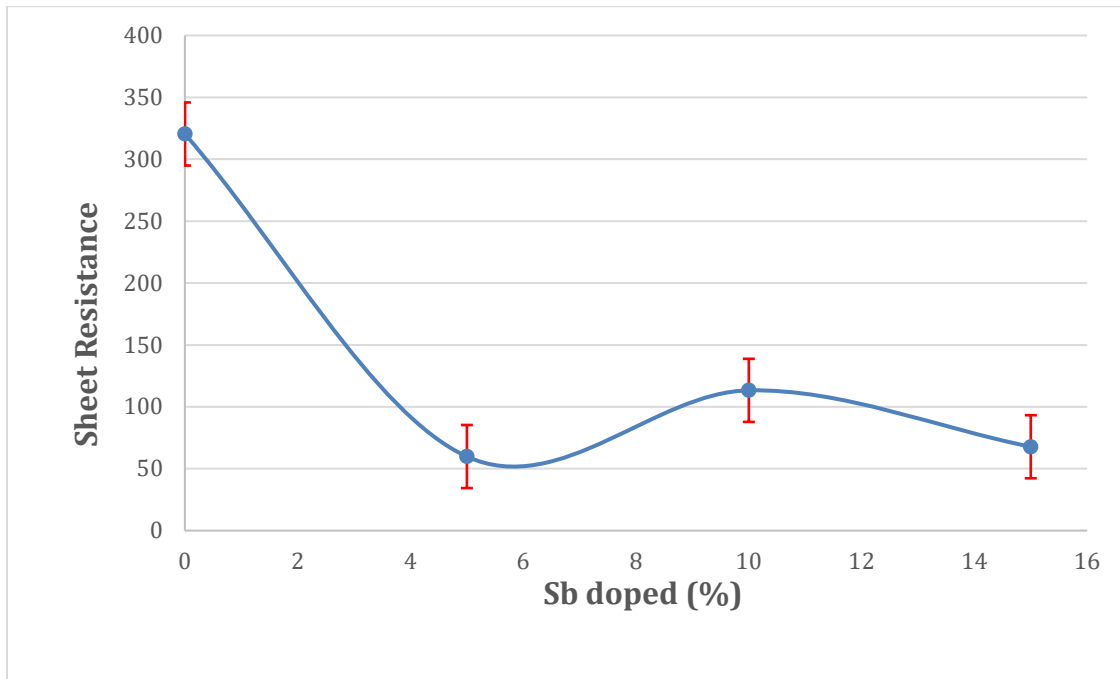


Figure 5.5 The influence of Sb doping on sheet resistance

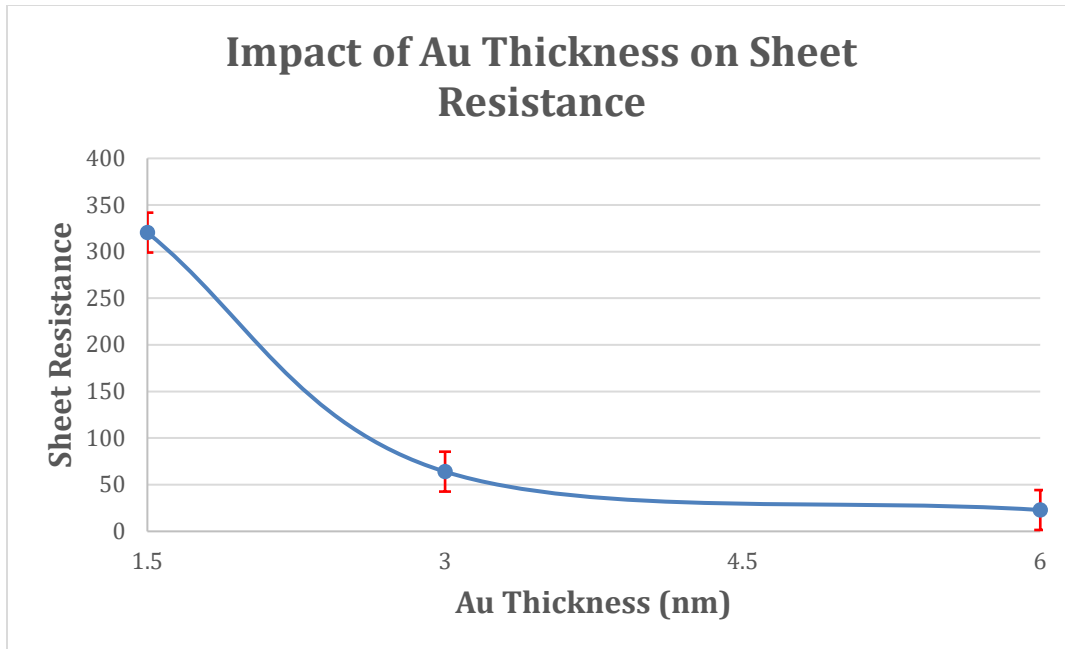


Figure 5.6 The influence of Au thickness on sheet resistance

It can be found that both Sb doping and Au thickness have an impact on the sheet resistance of the nanowire. There was a significant decrease of the sheet resistance when antimony was added. However, it seems the sheet resistance will not decrease when more and more antimony was added. This result may indicate that there is a limitation for Sb ions to incorporate into SnO₂ lattice. For Au thickness, the sheet resistance kept decreasing when the thickness increased.

5.1.3 The Influence on Optical Properties

The optical characteristics of the fabricated Sb-SnO₂ nanowire layers were examined by collecting diffuse reflectance spectrum with UV-vis spectrophotometer. The results were shown in figure 5.7. We can see from the UV results that the transmission decreases after doping with a fraction of antimony.

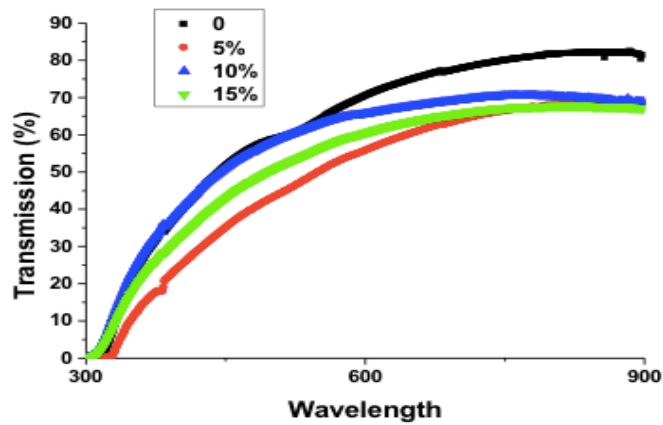


Figure 5.7. The influence of Sb doping on transmission

The transmission of nanowires grown on different thicknesses coated FTO layers were also checked by UV-vis spectrophotometer. Figure 5.8 exhibits the testing result. It can be found that the transmission decreased when the thickness of the coated gold increased.

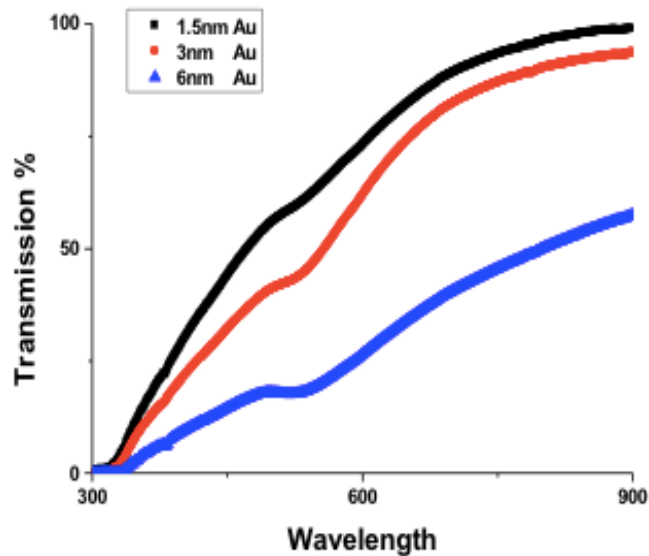


Figure 5.8. The influence of coated Au on transmission

5.1.4 Discussion about the Impact of Sb on Nanowire Morphology

It has not been figured out that why the doped antimony can increase the length and diameter of SnO₂ nanowire. In this thesis, several possible causes were discussed. One possible reason is the formation of solid solution $\text{Sn}^{4+}_{1-2x}\text{Sb}^{3+}_x\text{Sb}^{5+}_x\text{O}^{2-}_2$ during the nanowire growth process. The Sb incorporated into SnO₂ lattice has two different oxidation states, Sb³⁺ and Sb⁵⁺. The ratio of Sn⁴⁺, Sb³⁺ and Sb⁵⁺ may decide the lattice parameter of the oxide because the radii of these three ions are 0.69 Å, 0.76 Å and 0.61 Å respectively. Thus if the content of Sb³⁺ is high enough, the lattice parameter may be increased. In this way, the morphology of SnO₂ can be changed.

5.1.5 Impact of Sb Doping on Electrical/optical Properties of Nanowires

The effect of Sb dopants on the electrical and optical properties of nanowires is related to the mechanism of incorporation. The mechanism of how Sb ions incorporate into SnO₂ lattice has not been identified because of the lack of understanding of the incorporation process. [19] Trying to study this mechanism, several works were performed. Five different doping percent samples were checked by XRD and EDS: 0%, 2.5%, 5%, 10% and 15%.

Before showing the testing results, it is necessary to illustrate the theoretical assumption of Sb dopant's influence. As people know, SnO₂ is a classical n-type semiconductor so that oxygen vacancies are important for its conductivity. When Sb⁵⁺ ions incorporate into SnO₂ lattice, more oxygen vacancies are created, which will generate more electron carriers in the synthesized structures to increase the conductivity. On the other hand, three factors may affect the transmission: band gap, oxidation states and nanowire morphology. Burstein-Moss effect can be used as the theoretical assumption to explain the influence on band gap. When the doping

concentration is increased, the fermi level is pushed higher in energy from its original position, which lead to an increase of the apparent band gap. Another assumption is when an element is contained in the material with several different oxidation states or in mixed oxidation states, the light absorption will be enhanced. The reason is that electrons may transfer between two oxidation states of the same element, namely Sb^{3+} and Sb^{5+} in this thesis. That's why the decrease in the transmission of Sb-SnO₂ nanowires. The third factor is the morphology change of the nanowires. It has been proved in the previous experiments that the Sb dopant increase both the length and diameter of SnO₂ nanowires. That change can also be used to explain the decrease in the transmission.

The testing results of EDS is shown in figure 5.9.

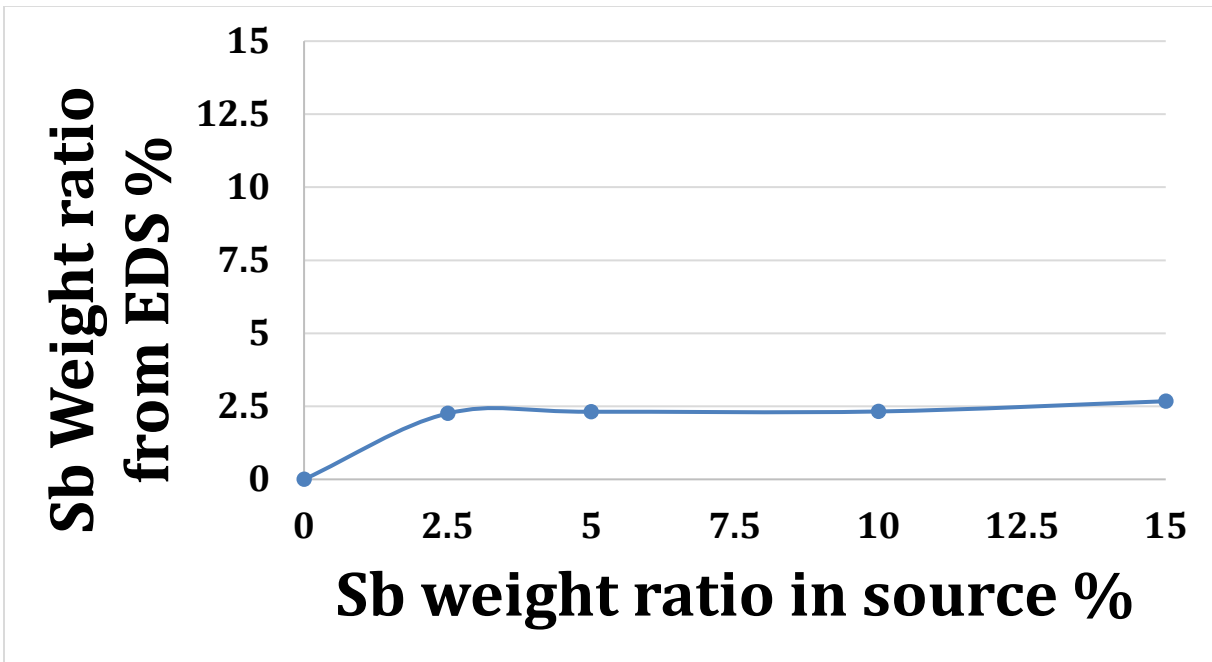


Figure 5.9. Sb concentration within SnO₂ nanowires by EDS when varying dopant concentration

It can be seen from the EDS results that there is a limitation for antimony to incorporate into SnO₂ lattice.

5.1.6 The Impact of Coated Gold on FTO Substrates

In VLS method of this thesis, gold layer is the prerequisite as it plays the role as catalyst. To study the influence of different thickness gold layer, pure gold layers deposited on FTO substrates by e-beam were annealed under the same condition of nanowire growth. Then the gold particles on the substrates were checked by SEM. SEM images of gold particles of the three different thicknesses layers are shown in figure 5.10.

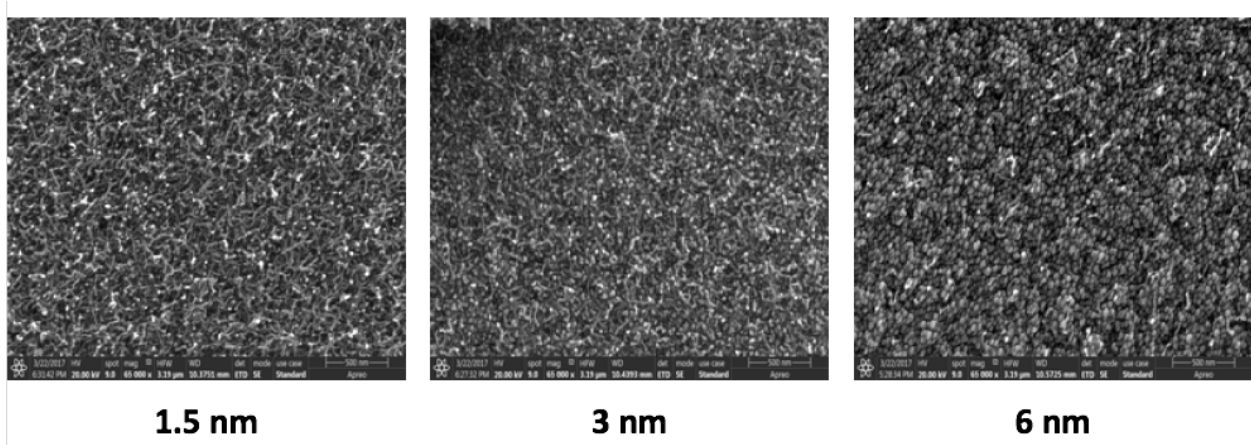


Figure 5.10. Au particles on different thickness gold layers

After measuring the size of the Au particles, the diameters of 1.5nm, 3nm and 6nm thickness gold particles are increased when the thickness increased. It has been illustrated in the previous part that gold is the required catalyst to grow nanowire and Au particles are on the tip of the nanowires. This may be the reason for the change of the nanowire morphology.

5.2 NANOWIRE BASED SUPERCAPACITOR

As mentioned previously, the grown SnO_2 nanowires were used as the substrates to fabricate supercapacitors. Manganese oxide and nickel oxide were deposited onto the nanowire layer by electrochemical deposition. Several factors were considered to influence the capacitance of the electrical capacitor such as scan rate of the deposition process, the weight ratio of electrolyte components and the substrates.

5.2.1 The Influence of the Supercapacitors

Jian Yan et al. has illustrated that the ideal structure of the fabricated electrical capacitor was a kind of “core-shell” structure. [2] This structure can be shown in Fig 5.11, tin oxide nanowire is covered by manganese oxide layer.

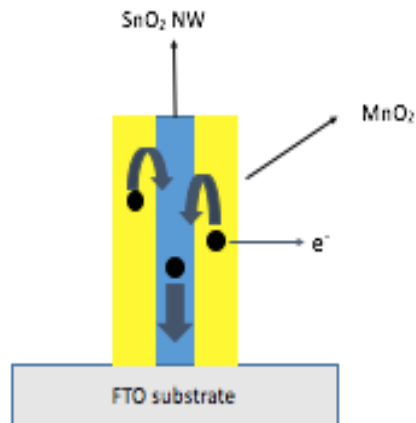


Figure 5.11. Ideal core-shell structure

It's meaningful to fabricate this nanostructure because of several advantages: (1) a thin layer of MnO_2 would enable a fast, reversible faradic reaction and provide a short ion diffusion path; (2) SnO_2 nanowires, with high conductivity, would provide a direct path for the electrons transport; and (3) SnO_2 nanowires would create channels for the effective transport of electrolyte.

5.2.2 The Nanostructure of the Capacitors

In this thesis, two different kinds of nanostructures were achieved due to two different voltage range for deposition. Figure 5.12 shows the two different structure of the deposited manganese oxide and nickel oxide.

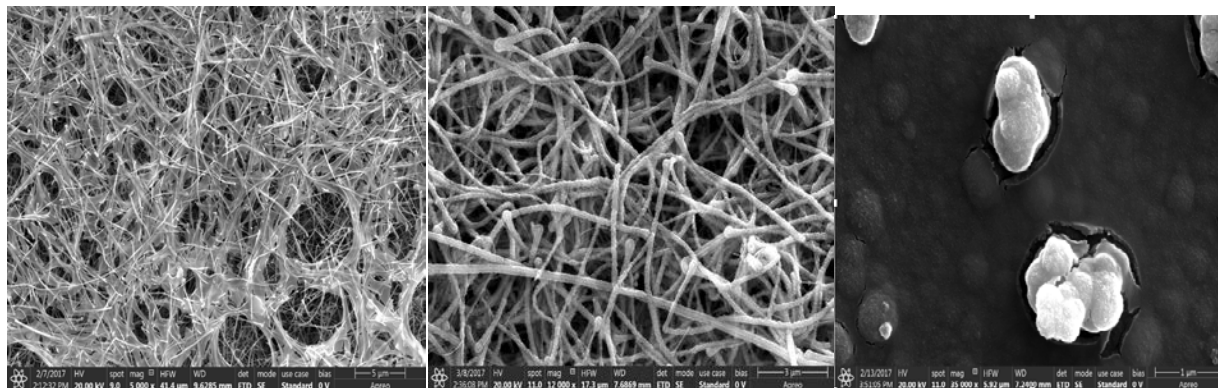


Figure 5.12. (a) nanostructure of manganese oxide with voltage 0-1 V; (b) nanostructure of manganese oxide with voltage range 0.4-1.2 V; (c) manganese oxide deposited on FTO

According to figure 5.12 (c), the nanostructure of manganese oxide deposited on pure FTO looks like nanoparticles. Thus the nanostructure of manganese oxide deposited on nanowire is related with the structure of nanowire. From the SEM images Fig 5.12 (a), it can be seen that

there was a structure which was like a thin film formed on the top of SnO₂ nanowire when the deposition voltage range was 0-1 V. However, when the voltage range was 0.4-1.2 V, the core-shell structure was formed (Fig 5.12 (b)). It can be found that SnO₂ nanowires were covered by a bright and thin layer, suggesting a core-shell structure. This thin shell layer is assumed to be manganese oxide and nickel oxide. To ensure the core-shell structure is formed, manganese and nickel oxides were deposited on shorter and more vertical nanowires which can be synthesized by decreasing the growth time of nanowire. Fig 5.13 shows the nanostructure of this method. It can be seen that all nanowires were coated and there is no thin pure nanowire being exposed.

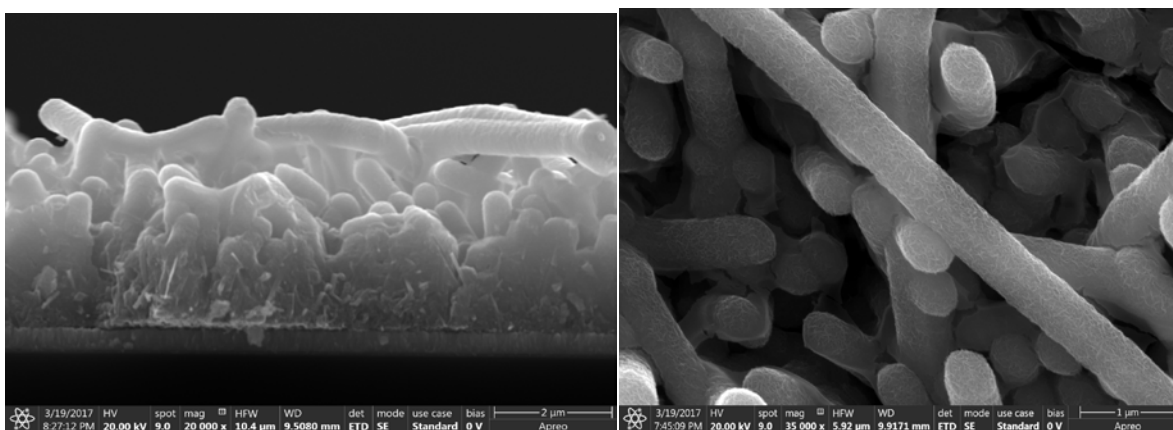


Figure 5.13. Deposited layer on short nanowires

The total thickness of TiO₂ nanoparticle/perovskite layer in figure 5.7(a) is around 500 nm, where TiO₂ nanoparticle layer is only 200 nm thick. The 300 nm thick perovskite layer refers to the cuboid structure. [34] The crystal size of cuboid crystal is in a negative relationship with the concentration of MAI solution, which is 7 mg/mL (0.044 M) in this experiment. In principle, 0.044 M MAI solutions can produce perovskite crystal with grain size around 300 nm. [34] The hysteresis of I-V curve scanning direction is also related to the size of cuboid crystal.

When the cuboid is produced by low concentration MAI, the dependency can be ignored. On the contrary, the dependency is significant. [34] Besides, crystalline perovskite infiltrates the mesoporous TiO₂ and results in miscellaneous order of perovskite and TiO₂ in the light absorber layer. Figure 5.7(b) shows no explicit perovskite cuboid layer occurs on top of TiO₂ nanowire structure. The thickness of TiO₂/perovskite is around 600 nm, which is similar to the thickness in nanoparticle based PSC sample. TiO₂ nanowire and perovskite are well aligned in the light absorber layer. In TiO₂ nanoparticle based PSC, the HTM layer infiltrated in the interspace of perovskite cuboid crystal grains, while in TiO₂ nanowire based PSC, the HTM layer (dark) is explicit located on the top of TiO₂/perovskite layer. In addition, the thin layer on the top of the samples is Au electrode.

The concentrations of Manganese and nickel are measured by EDS. The testing results of two different structures shown in figure 5.14 and 5.15.

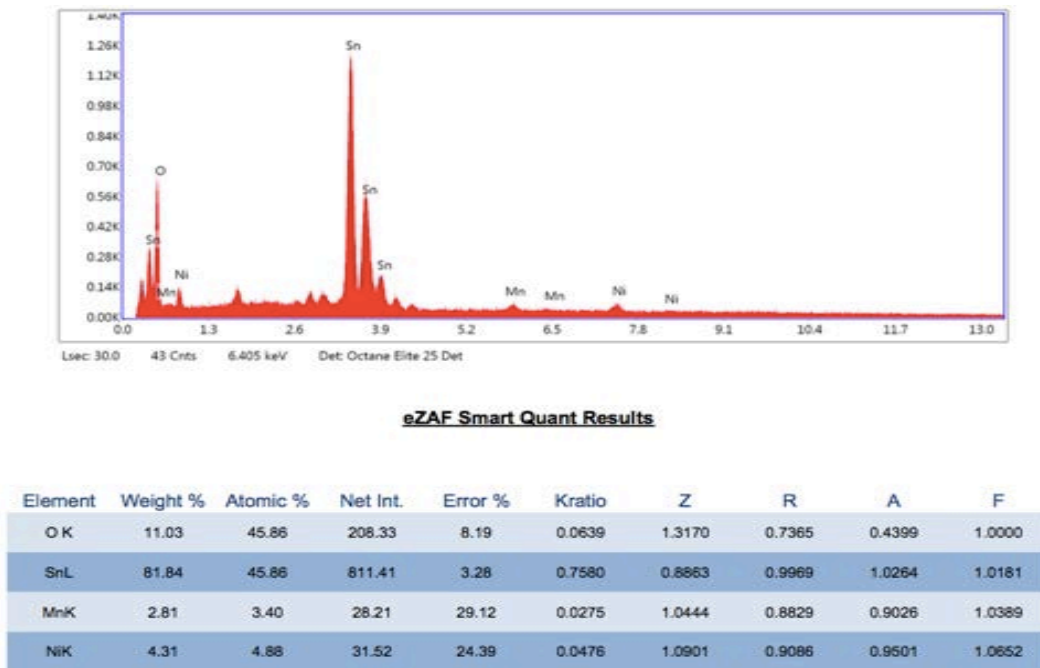
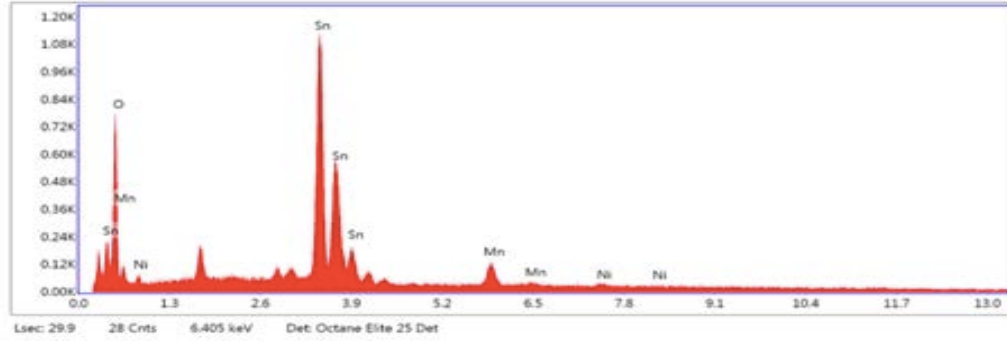


Figure 5.14. Concentration of low voltage range



eZAF Smart Quant Results

Element	Weight %	Atomic %	Net Int.	Error %	Kratio	Z	R	A	F
O K	13.07	49.50	253.96	7.85	0.0778	1.3006	0.7476	0.4580	1.0000
SnL	76.39	39.01	751.83	3.33	0.7023	0.8756	1.0109	1.0306	1.0188
MnK	8.71	9.60	86.62	11.26	0.0846	1.0309	0.8940	0.9099	1.0361
NiK	1.84	1.89	13.23	56.47	0.0200	1.0748	0.9188	0.9503	1.0650

Figure 5.15. Concentration of high voltage range

5.2.3 The Possible Mechanism

This deposition process is due to a series of chemical reactions. Several equations can be presented to describe the fabrication of the two metal oxides via electrochemical deposition. In the three electrodes system, H₂O will be reduced on the working electrode when the potential is applied to the system. This process can be described by Equation 5.1.



Because of the reduction of water, more OH⁻ ions are provided in the system. OH⁻ ions are considered to be the vital factor in this deposition because the condensation of metal ions (Mn⁺ and Ni⁺) occurs where the OH⁻ were localized. The combination of metal cations and OH⁻ ions leads to the nucleation of metal hydroxide. After annealing process, these metal hydroxides will be oxidized to become metal oxides, as described by equation 5.2 and 5.3.





The nucleation and growth of the metal oxide may be affected by several factors such as different deposition voltage range in this thesis. This is still needed to be discussed in the future.

5.2.4 Electrical Behavior Characterization

To determine the electrical capacitance of the fabricated capacitor, cyclic voltammetry was performed in 0.5 M sodium sulfate solution in a potential window ranging from 0 to 1 V at a scan rate of 20 mV/s. It is notable that the measured capacitance was mostly resulted from coated metal oxides and the contribution of nanowire is negligible. There are two reasons to support this conclusion. The first one is the core-shell structure. The SnO₂ nanowires were coated with a thin layer so that they could not take part into the charge storing process immediately. The charge was stored at or near the surface of the electrode material during the faradic reactions. The second reason is the measured electrical capacitance of pure SnO₂ nanowires was very low, compared with the capacitance of the deposited samples. The possible mechanism of the testing process can be described by equation 5.4 and 5:



From the equations above, it can be found that OH⁻ ions play an important role in charge storage. Decreasing the concentration of OH⁻ ions in the electrolyte solution may lead to less contributions from metal oxide redox reactions.

5.2.5 The Influence of Deposition Scan Rate

The electrical capacitance of the deposited layer was measured by three electrodes system with cyclic voltammetry method. In this research, the mass of the deposited layer cannot be achieved accurately because of the lack of accurate microbalance. The mass of the MnO_2/NiO can be rough estimated to be $100\ \mu\text{g}$ so that the specific capacitance can be rough calculated. The CV curves and specific capacitances with different deposition scan rates are shown in figure 5.16.

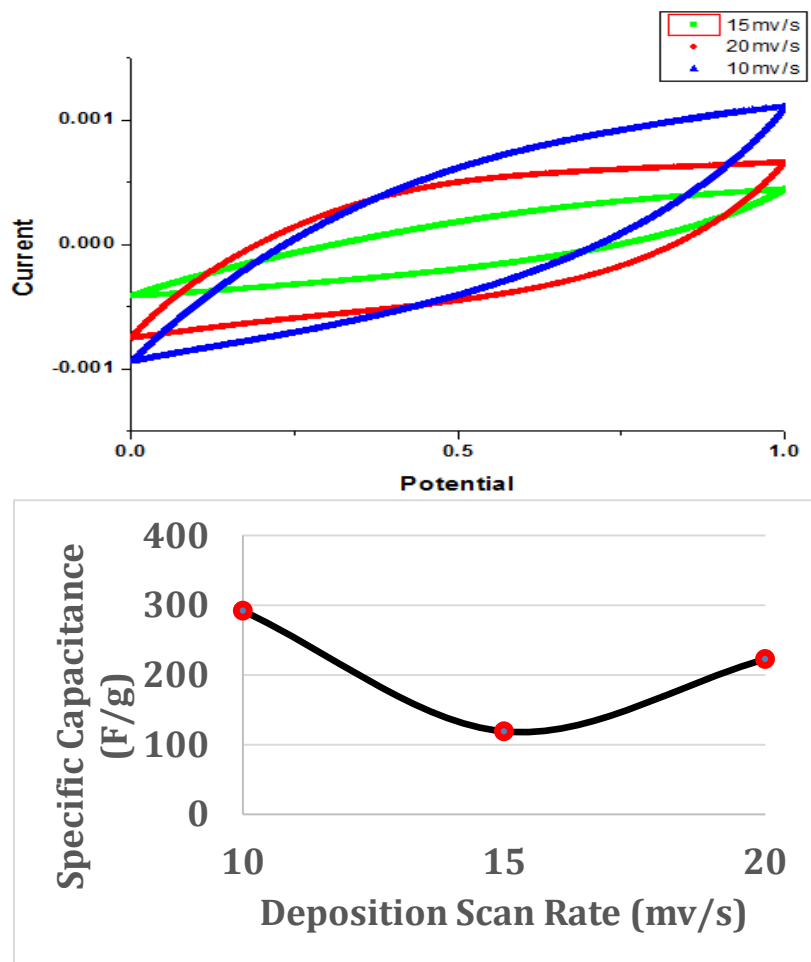


Figure 5.16. CV curves and specific capacitance under different deposition scan rates

In this thesis, the deposition scan rate didn't show a regular influence and scan rate of 10mv/s exhibits high specific capacitance.

5.2.6 The Influence of Mn/Ni Oxide Ratio

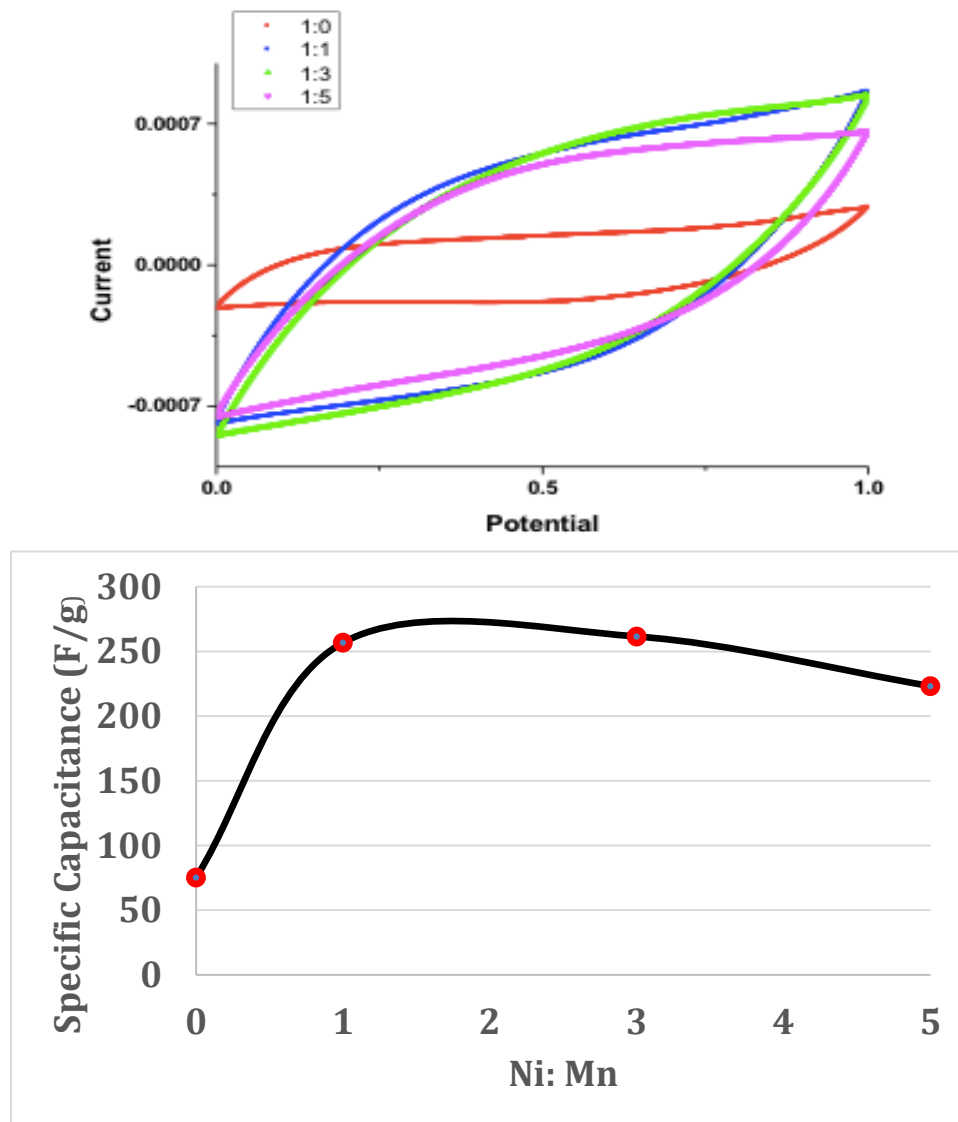


Figure 5.17. CV curves and specific capacitance of different NiO content samples

Pure MnO_2 and MnO_2/NiO composite were checked by CH instrument. During the deposition process, different ratio of nickel acetate tetrahydrate was added into the electrolyte to fabricate the pseudocapacitors. Figure 5.17 showed the CVs and specific capacitances of these materials. It can be seen that the composite has a much higher specific capacitance than MnO_2 . However, different ratio of NiO show similar specific capacitance. To explain the effect of NiO, it's necessary to understand the drawback of MnO_2 . The limitation of MnO_2 material's capacity may due to its large resistivity and the equivalent series resistance (ESR). [32] The composite electrode materials based on manganese oxide are prepared to overcome this disadvantage. The increase of the specific capacitance may be due to the synergic effects from each component. In addition, higher electrochemical stability which leads to more available active site could be also a reason to improve the capacity of MnO_2 electrode.

5.2.7 The Results of Different Measuring Scan Rate

When measuring the CV curves of fabricated capacitors, the results varied from scan rates. The CV curves was shown in figure 5.18.

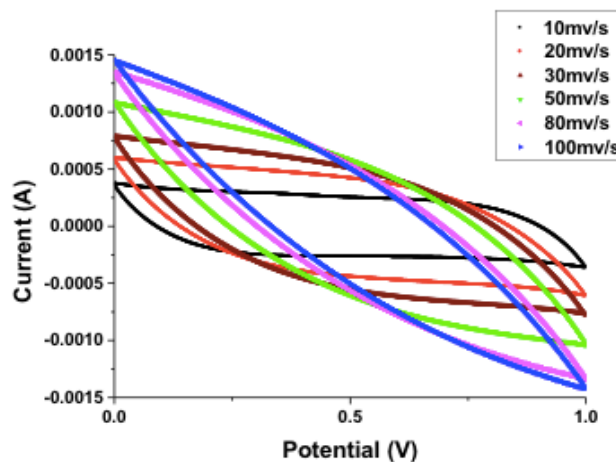


Figure 5.18. CV curves of various measuring scan rates

The specific capacitance results were shown in figure 5.19.

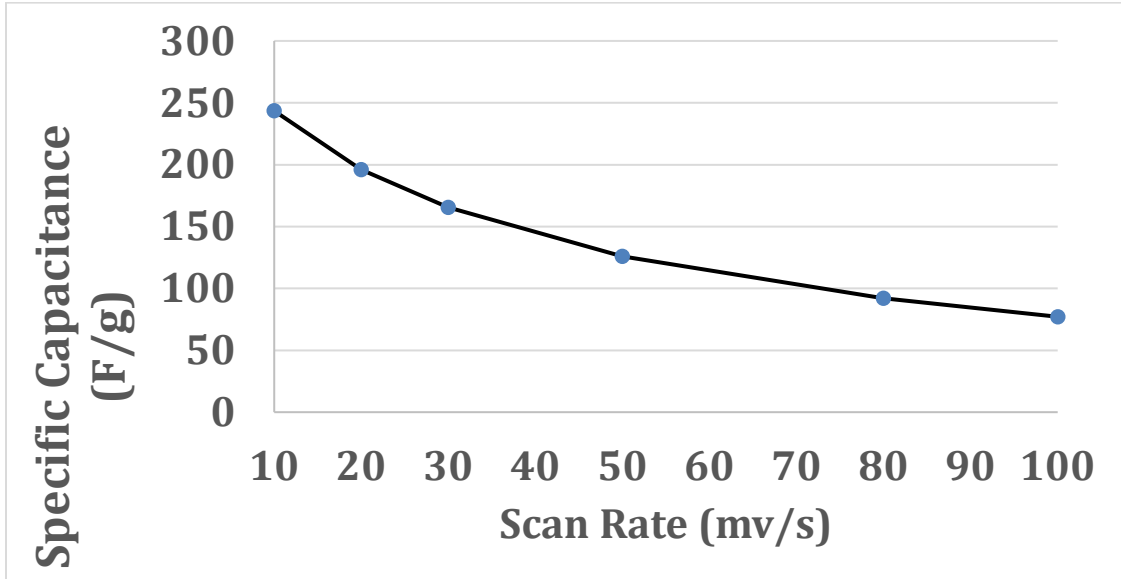


Figure 5.19. Specific capacitances under different scan rates

It can be seen that the specific capacitance decreased when the scan rate increased and the max value was nearly 250 F/g. Low scan rate may lead to higher capacitance value, the best sample of the research is expected to have a high specific capacitance.

5.3 NANOWIRE GROWN ON MESH

Stainless steel mesh was also used as the substrate for nanowire growth in this thesis. Some mesh substrates were coated with gold before the grown process while the others not. It can be found from the SEM images (figure 5.20) that SnO₂ nanowires were successfully grown on both of gold coated mesh and pure SS mesh without gold coated.

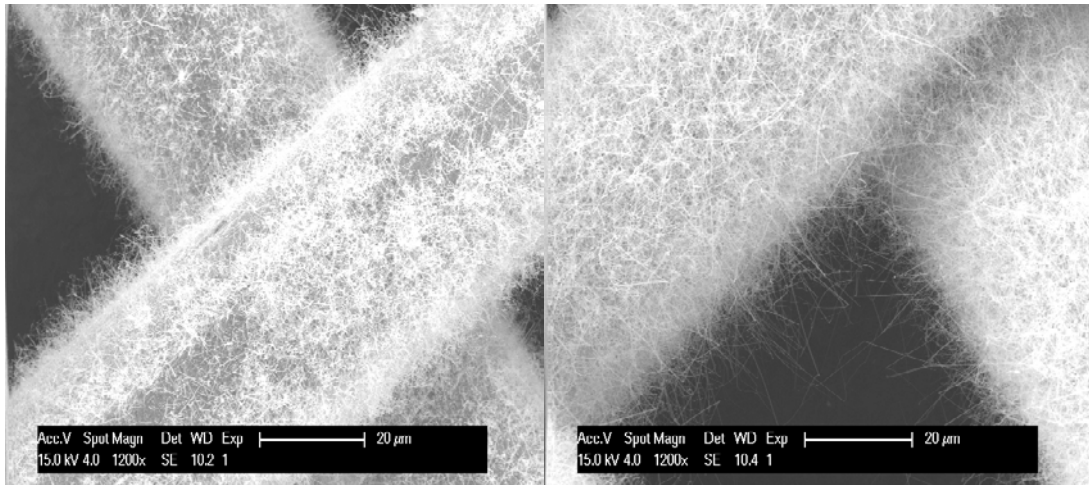


Figure 5.20. Nanowire grown on (a) pure SS mesh; (b) gold coated SS mesh

Though nanowire can grow of both pure and coated mesh substrates, the morphology and density of nanowires were different, obviously. The density of nanowire was much higher when the mesh substrates were coated with gold. In addition, the temperature may also have an impact on the density. By comparing the samples with temperature difference, we can achieve that the density would decrease under a lower growing temperature. As for the nanowire morphology, software ImageJ was used to measure the diameter and length of the nanowire and the results were shown in figure 5.21.

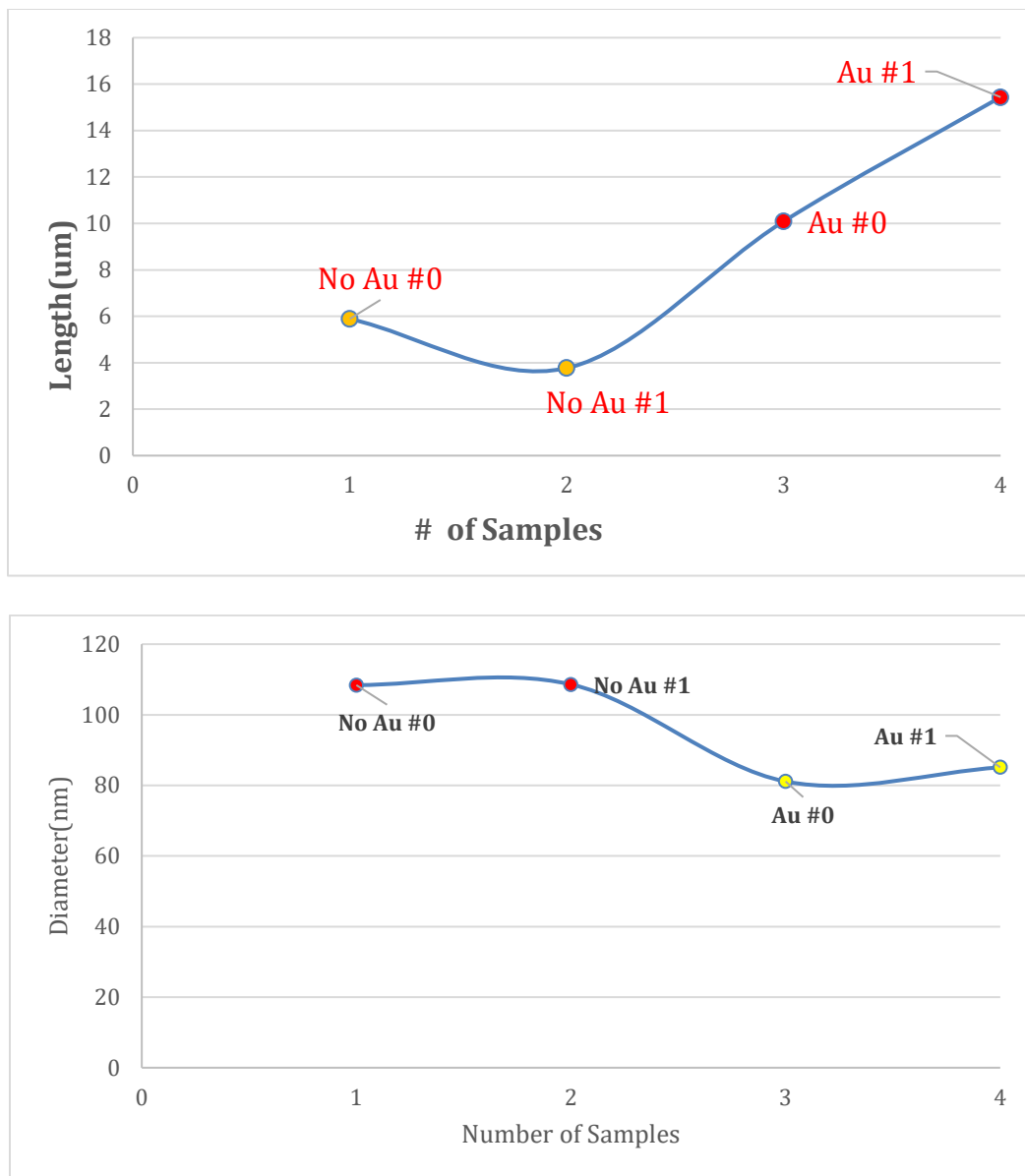


Figure 5.21. (a) The lengths of nanowires grown on mesh; (b) The diameters of nanowires grown on mesh

According to the measurement, nanowires grown on pure mesh were shorter and thicker while nanowires grown on gold coated mesh were longer and thinner. Moreover, it seems nanowires grown under different temperature may have a different morphology. Due to the amount of mesh samples were not enough, these results are still waited to be ensured. More efforts are needed to be performed to come to an accurate conclusion.

6.0 CONCLUSION

The topic of this thesis is to deposit MnO_2/NiO layer onto SnO_2 nanowires to form a core-shell structure pseudocapacitor by electrochemical deposition.

The first step of the entire process is to grow uniform SnO_2 nanowires on FTO substrates via VLS method on 800 degree centigrade. To improve the properties of SnO_2 nanowires, antimony was used as dopant. SEM was used to check the morphology and structure of the grown nanowires. It was found that the Sb-doped nanowires were longer and wider than pure SnO_2 nanowires. The lengths of pure nanowires are ranging from 15 μm to 20 μm while the doped ones are ranging from 25 μm to 30 μm . The diameters of pure nanowires are ranging from 50 nm to 60 nm while the doped ones are ranging from 100 nm to 110 nm. The electrical and optical properties of both pure and doped nanowires were checked by four probe measurement and UV-vis spectroscopy, respectively. Sb dopant reduced the sheet resistance of nanowire layer from 400 Ω/sq to around 50 Ω/sq . In addition, the transmission of nanowires also decreased because of doping the antimony.

The thickness of coated gold layer on FTO substrates was also considered to be a parameter to influence the property and morphology of nanowires. The SEM images and the characterization of properties show the impact of gold layer. The nanowires grown on substrates coated with thicker gold layer were usually longer and thicker. This change in morphology was believed to be the main reason for the change of transmission. On the other hand, the

improvement of conductivity by increasing the Au thickness has not been identified. The increase of Au content in the tips of nanowires may be a potential reason.

Those grown SnO_2 nanowires were then used as the substrates to fabricate pseudocapacitors by depositing MnO_2 and NiO onto them. Core-shell structure was successfully formed by electrochemical deposition. The specific capacitances of the fabricated capacitors were checked by CHI66. The scan rate and nickel content were found to influence the specific capacitance. It can be found that MnO_2/NiO composite had higher specific capacitance than pure MnO_2 did. The specific capacitance of the fabricated capacitor can be rough estimated to be 250 F/g.

SnO_2 nanowires were also grown on stainless steel mesh for the future work. Differ from growing on FTO substrates, nanowires can grow on SS mesh without Au catalyst. However, nanowires grown on Au coated mesh seem more uniform and dense. These mesh samples are going to be as substrates to fabricate new kinds of pseudocapacitors.

REFERENCES

- [1] “Transparent metallic Sb-doped SnO₂ nanowires” Qing Wan, Eric N. Dattoli, and Wei Lu, *Appl. Phys. Lett.* 90, 222107 (2007)
- [2] “Facile coating of Manganese Oxide on Tin Oxide Nanowire with High-performance Capacitive Behavior” Jian Yan, Eugene Khoo, Afriyanti Sumboja, and Pool See Lee, American Chemical Society, Published July 1, 2010.
- [3] “A facile synthesis of α -MnO₂ used as a supercapacitor electrode material: The influence of the Mn-based precursor solutions on the electrochemical performance” Wenyao Li, Jiani Xu, Yishunag Pan, Lei An, Kaibing Xu, Guangjin Wang, Zhishui Yu, Li Yu, Junqing Hu, *Applied Surface Science* 357 (2015)
- [4] “Effects of Electrodeposition Mode and Deposition Cycle on the electrochemical Performance of MnO₂-NiO Composite Electrodes for High-Energy-Density Supercapacitors” Rusi, S.R. Majid, *PLOS one*, May 16, 2016
- [5] “Morphological changers and electrochemical response of mixed nickel manganese oxide as charge storage electrodes” Tuyen Nguyen, Michel Boudard, Laetitia Rapenne, M. Joao Carmezim and M. Fatima Montemor, *Journal of Materials Chemistry A*, 2015, 3.
- [6] “Nanoflake Manganese Oxide and Nickel-Manganese Oxide Synthesized by Electrodeposition for Electrochemical Capacitor” Man Van Tran, An The Ha, and Phung My Loan Le, *Journal of Nanomaterials* Volume 2015
- [7] “Nanosized Mn-Ni oxide thin film via anodic electrodeposition: a study of the correlations between morphology, structure and capacitive behavior” Mohammad H. Tahmasebi, Antonello Vincenzo, Mazdak Hashempour, Massimiliano Bestetti, Mohammad A. Golozar, Keyvan Raeissi, *Electrochimica Acta* 206 (2016)
- [8] “High performance super-capacitive behavior of deposited manganese oxide/nickel oxide binary electrode system” Rusi, S.R. Majid, *Electrochimica Acta* 138 (2014)
- [9] “Large-Scale Synthesized and Microstructure of SnO₂ Nanowires coated with Quantum-Sized ZnO Nanocrystals on a Mesh Substrate” Weidong Yu, Xiaomin Li, Xiangdong Gao, and Feng Wu, *J. Phys. Chem. B* 2005

- [10] “An excellent enzyme Biosensor based on Sb-doped SnO₂ nanowires” Limiao Li, Jin Huang, Taihong Wang, Hao Zhang, Yang Liu, Jinghong Li, *Biosensors and Bioelectronics* 25 (2010)
- [11] “Single-crystalline Sb-doped SnO₂ nanowires: synthesis and gas sensor application” Q. Wan and T.H. Wang, *Chem. Commun.*, 2005
- [12] “Branched growth of degenerately Sb-doped SnO₂ nanowires” Jin Huang, Aixia Lu, Bin Zhao, and Qing Wan, *Applied Physics Letters* 91, 073102(2007)
- [13] “Materials Science Manufacturing” Rajiv Asthana, Ashok Kumar and Narendra Dahotre
- [14] “Doping-Dependent Electrical Characteristics of SnO₂ Nanowires” Qing Wan, Eric Dattoli, and Wei Lu, *Small* 2008
- [15] “Tailoring the pseudocapacitive behavior of electrochemically deposited manganese-nickel oxide films” Mohammad H. Tahmasebi, Keyvan Raeissi, Mohammad A Golozar, Antonello Vincenzo, Mazdak Hashempour, Massimiliano Bestetti, *Electrochimica Acta* 190 (2016)
- [16] “Characterizing and comparing the cathodoluminescence and field emission properties of Sb doped SnO₂ and SnO₂ nanowires” Jyh-Ming Wu, *Science Direct Thin Solid Films* 517 (2008)
- [17] “A room temperature ethanol sensor made from p-type Sb-doped SnO₂ nanowires” Jyh Ming Wu, *Nanotechnology* 21 (2010)
- [18] “Tin doped indium oxide core-TiO₂ shell nanowires on stainless steel mesh for flexible photoelectrochemical cells” Jun Hong Noh, Bo Ding, Hyun Soo Han, Ju Seong Kim, Jong Hoon Park, Sang Baek Park, Hyun Suk Jung, Jung-Kun Lee, and Kug Sun Hong, *Applied Physics Letters* 100 (2012)
- [19] “Crucial role of doping dynamics on transport properties of Sb-doped SnO₂ nanowires” Annop Klamchuen, Takeshi Yanagida, Kazuki Nagashima, Shu Seki, Keisuke Oka, Masateru Taniguchi, and Tomoji Kawal, *Appl. Phys. Lett.* 95 (2009)
- [20] “Conductive SnO₂/Sb powder: preparation and optical properties” Z.CRNJAK, B. OREL, M. HODOSCEK et al. *Journal of materials science* 27 (1992)
- [21] “A Thermodynamic Study of Phase Equilibria in the Au-Sb-Sn Solder System” Jong Hoon Kim, Sang Won Jeong, and Hyuck Mo Lee, *Journal of ELECTRONIC MATERIALS*, Vol. 31, No. 6, 2002
- [22] https://en.wikipedia.org/wiki/Cyclic_voltammetry

- [23] “Phase Equilibria of the Sn-Sb Binary System” Sinn-Wen Chen, Chih-Chi Chen, Wojcieh Gierlitka, An-Ren Zi, Po-Yin Chen, Hsin-Jay Wu, Journal of Electronic Materials July 2008, Volume 37
- [24] “VAPOR-LIQUID-SOLID MECHANISM OF SINGLE CRYSTAL GROWTH” R.S.Wagner and W.C.Ellis, Aool.Phys. Lett. 4, 89 (1964)
- [25] “A new proposal for the binary (Sn, Sb) phase diagram and its thermodynamic properties based on a new e.m.f. study” V. Vassiliev, M. Lelaurain, J. Hertz Journal of Alloys and Compounds, Vol. 247 1997
- [26] “Structural studies of nanocrystalline SnO₂ doped with antimony: XRD and Mossbauer spectroscopy” B. Grzeta et al. Journal of Physics and Chemistry of Solids 63 (2002)
- [27] “Metal to insulator transition in Sb doped SnO₂ monocrystalline nanowire thin films” I. M. Costa, E. P. Bernardo, B. s. Marangoni, E. R. Leite, and A. J. Chiquito, Journal of Applied Physics 120 (2016)
- [28] “Applications and Processing of Transparent Conducting Oxides” brian G. Lewis and David C. Paine
- [29] “Band Theory of Solids” <http://hyperphysics.phy-astr.gsu.edu>
- [30] “Patent US6559941-UV-vis Spectrophotometry” Google books, N.p, n.d. Web. 28 2016
- [31] “Microwave-driven Synthesis of Iron Oxide Nanoparticles for Fast Detection of Atherosclerosis | Protocol” Microwave-driven Synthesis of Iron Oxide Nanoparticles for Fast Detection of Atherosclerosis | Protocol. N. P., n.d. 2016
- [32] “Preparation and characterization of nanostructured NiO/MnO₂ composite electrode for electrochemical supercapacitors” En-Hui Liu, Wen Li, Jian Li, Xiang-Yun Meng, Rui Ding, Song-Ting Tan, Materials Research Bulletin 44 (2009)
- [33] “Manganese oxide –based materials as electrochemical supercapacitor electrodes” Weifeng Wei, Xinwei Cui, Weixing Chen and Douglas G. Ivey, Chem. Soc. Rev., 2011
- [34] “Transparent Conducting Oxides-Au Up-To-Date Overview” Research Gate. Web. 28 Mar 2016
- [35] “Study of Transparent Indium Tin Oxide for Novel Optoelectronic Devices” OpenGrey. Mar. 2016
- [36] “Cyclic Voltammetry” Peter T. Kissinger, William R. Heineman
- [37] “Photovoltaics for the 21th century” V.K. Kapur, R.D. McConnell, D. Carlson, G.P. Ceasar, A.Rohatgi

- [38] “Evaluation of bulk and surface absorption edge energy of sol-gel-dip-coating SnO₂ thin films” Emerson Aparecido Floriano et al. Mat. Res. Vol. 13 2010
- [39] “Supercapacitor (EDLC) Basics” Part 1
- [40] http://people.clarkson.edu/~droy/Corrosion_EIS.htm
- [41] <https://en.wikipedia.org/wiki/Pseudocapacitance>
- [42] “Novel co-evaporation approach for the growth of Sb doped SnO₂ nanowires” R. Rakesh Kumar, K. Narasimha Rao, K. Rajanna, A.R. Phani, Materials Letters Vol 106 2013
- [43] <http://four-point-probes.com/four-point-probe-manual/>
- [44] http://people.clarkson.edu/~droy/Corrosion_EIS.htm